MR Imaging of Muscle Trauma: Anatomy, Biomechanics, Pathophysiology, and Imaging Appearance[1]

Dyan V. Flores, MD
Catalina Mejía Gómez, MD
Mauricio Estrada-Castrillón, MD
Edward Smitaman, MD
Mini N. Pathria, MD

Abbreviations: CECS = chronic exertional compartment syndrome, DOMS = delayed-onset muscle soreness, MTJ = myotendinous junction

RadioGraphics 2018; 38:0000–0000

https://doi.org/10.1148/rg.2018170072

Content Codes: ER MK MR

[1]From the Department of Radiology, Philippine Orthopedic Center, Maria Clara Street, Santa Mesa Heights, Quezon City, Metro Manila, Philippines 1100 (D.V.F.); Department of Radiology, Hospital Pablo Tobón Uribe, Medellín, Colombia (C.M.G., M.E.C.); and Department of Radiology, UCSD Medical Center, San Diego, Calif (E.S., M.N.P.). Recipient of a Certificate of Merit award for an education exhibit at the 2016 RSNA Annual Meeting. Received March 30, 2017; revision requested July 26 and received August 14; accepted September 12. For this journal-based SA-CME activity, the authors, editor, and reviewers have disclosed no relevant relationships. **Address correspondence to** D.V.F. (e-mail: *dyanflores@yahoo.com*).

SA-CME LEARNING OBJECTIVES

After completing this journal-based SA-CME activity, participants will be able to:

- Recognize the typical MR imaging appearance of a wide range of acute, subacute, and chronic traumatic muscle disorders commonly encountered in clinical practice.
- Understand how different types of muscle injuries relate to the biomechanics, pathophysiology, and—most important—anatomy of the muscle.
- Describe the MR imaging findings that most accurately reflect the severity of the injury in the comprehensive grading systems used for guiding rehabilitation in the injured athlete.

See www.rsna.org/education/search/RG.

Muscle is an important component of the muscle-tendon-bone unit, driving skeletal motion through contractions that alter the length of the muscle. The muscle and myotendinous junction (MTJ) are most commonly injured in the young adult, as a result of indirect mechanisms such as overuse or stretching, direct impact (penetrating or nonpenetrating), or dysfunction of the supporting connective tissues. Magnetic resonance (MR) imaging is widely used for assessment of muscle injuries. This review illustrates the MR imaging appearance of a broad spectrum of acute, subacute, and chronic traumatic lesions of muscle, highlighting the pathophysiology, biomechanics, and anatomic considerations underlying these lesions. Concentric (shortening) contractions are more powerful, but it is eccentric (lengthening) contractions that produce the greatest muscle tension, leading to indirect injuries such as delayed-onset muscle soreness (DOMS) and muscle strain. Strain is the most commonly encountered muscle injury and is characteristically located at the MTJ, where maximal stress accumulates during eccentric exercise. The risk of strain varies among muscles based on their fiber composition, size, length, and architecture, with pennate muscles being at highest risk. Direct impact to muscle results in laceration or contusion, often accompanied by intramuscular interstitial hemorrhage and hematoma. Disorders related to the muscle's collagen framework include compartment syndrome, which is related to acute or episodic increases in pressure, and muscle herniation through anatomic defects in the overlying fascia. The healing response after muscle trauma can result in regeneration, degeneration with fibrosis and fatty replacement, or disordered tissue proliferation as seen in myositis ossificans. In athletes, accurate grading of the severity and precise location of injury is necessary to guide rehabilitation planning to prevent reinjury and ensure adequate healing. In elite athletes, MR imaging grading of muscle trauma plays an increasingly important role in recently developed comprehensive grading systems that are replacing the imprecise three-grade injury classification system currently used.

Introduction

Muscle injury is common, often occurring during sports, affecting the athlete's functional capacity and ability to continue. Acute muscle injuries are classified by the mechanism of injury into strain caused by indirect stretching, contusion after a direct blow, laceration resulting from penetrating trauma, and compartment syndrome arising from elevated pressure (1–4). While clinical classification systems primarily emphasize only acute forms of muscle trauma, radiologists also need to be familiar with a range of subacute and

TEACHING POINTS

- Muscle is the motor driving the muscle-tendon-bone unit, affording movement and locomotion. The location of failure in this unit after injury varies with age, occurring predominantly at the bone in younger individuals with open physes, in the muscle and myotendinous junction (MTJ) in young adults, and at the tendon in older individuals with preexisting tendon degeneration.
- Muscle strain related to stretching is the most commonly imaged muscle injury, localizing to the MTJ, which has limited ability to tolerate forces generated during eccentric contraction. The risk of strain is highest in muscles that are large, cross two articulations, contain a high proportion of type 2 muscle fibers, and exhibit pennate architecture.
- Muscle contusion caused by a direct blow to the muscle results in an admixture of focal hematoma and interstitial hemorrhage at the site of impact of variable signal intensity at MR imaging, depending on the stage of blood product degradation. Differentiation from neoplasm in patients lacking a clear history of injury can be challenging; following the lesion to document temporal resolution is recommended in such patients.
- The muscle wrappers consist of supporting connective tissue; they organize and protect the muscle tissue but restrict its ability to expand. Fascial envelopes form confined muscle compartments that can be damaged if pressure within the compartment is increased. Acute compartment syndrome after trauma is infrequently imaged, as muscle can become necrotic if the condition is not promptly treated. However, imaging may play a role in diagnosis of chronic exertional compartment syndrome.
- Recently, several comprehensive grading systems for muscle injury in athletes have been developed that incorporate MR imaging assessment regarding the dimensions, morphology, and precise location of the injury. Preliminary findings suggest that these more complex grading systems afford more accurate prognostication regarding return to play than the simpler three-grade classification system typically employed by radiologists.

chronic injuries that can result in symptoms and functional limitation (Table 1).

Radiography and computed tomography (CT) are excellent for identifying fractures and soft-tissue mineralization but play a limited role in imaging acute muscle injury. Magnetic resonance (MR) imaging and ultrasonography (US) have excellent spatial and soft-tissue contrast resolution, enabling detailed evaluation of muscle and its connective tissue framework. US is widely available and affords dynamic evaluation but is less sensitive for low-grade muscle injury and more operator dependent. MR imaging is widely used for assessment of muscle trauma, particularly in the high-performance athlete, affording simultaneous evaluation of soft tissues and osseous structures. It plays an increasingly important role in grading injury severity and guiding return to play in the injured athlete.

Novel techniques such as diffusion tensor imaging and MR spectroscopy can be employed to obtain quantitative information in muscle injury. Diffusion tensor imaging can demonstrate microstructural disorganization related to damaged muscle tissues causing disruption of normal preferential diffusion along muscle tracks (5). A postexercise deficit in oxygen saturation that correlates with increased muscle compartment pressure can be quantified with near-infrared spectroscopy (6,7).

In this article, we define and illustrate the spectrum of traumatic muscle disorders commonly encountered in clinical practice, emphasizing MR imaging features and highlighting the relationship of muscle function, biomechanics, anatomy, and architecture to muscle trauma.

Muscle Organization and Function

The function of skeletal muscle is to act as the engine or "motor" driving the muscle-tendon-bone unit, affording movement and locomotion. This unit is a highly organized complex of tissues consisting of the following: *(a)* the muscle; *(b)* the myotendinous junction (MTJ), where muscle fibers interdigitate with the tendon and epimysium; *(c)* the tendon, which may be at the ends of and/or within the muscle; *(d)* the enthesis, where the tendon attaches to the bone; and *(e)* the bone (8) (Fig 1).

Muscle tissue is organized by a stroma of connective tissue that wraps muscle cells together into progressively larger longitudinally oriented units (9). The cellular unit of muscle is the muscle fiber, which is wrapped by a collagenous envelope known as endomysium. A group of muscle fibers makes up a muscle fascicle, which is wrapped by perimysium. A group of fascicles makes up the muscle itself, which is wrapped by epimysium (Fig 2). A group of muscles enclosed by connective tissue fascia is referred to as a compartment. Muscles within a compartment typically have similar function in terms of limb movement and a shared peripheral nerve supply.

Failure of any component of the muscle-tendon-bone unit can result in breakdown of movement, and the location of tissue failure varies depending on patient age (3). A normal healthy tendon is the strongest link in the muscle-tendon-bone unit and is rarely injured. It is only in older patients, after the tendon has degenerated and weakened, that it becomes the primary site of failure (Fig 3) (10,11). In the child or adolescent with open physes, failure tends to occur at the bone, resulting in fracture, physeal avulsion, or periosteal injury (Fig 4). It is in the young skeletally mature adult with healthy tendons that failure predominantly occurs at the MTJ and in the muscle (Fig 5).

Table 1: Classification of Muscle Injury

Presentation	Trauma Mechanism	Injury
Acute	Indirect	Myotendinous junction (MTJ) strain
	Direct	Contusion with acute hemorrhage Laceration
	Related to fascia	Acute compartment syndrome
Delayed/ subacute	Indirect	Delayed-onset muscle soreness (DOMS)
	Direct	Subacute hematoma
Chronic	Indirect	Disordered healing with fibrosis/atrophy
	Direct	Chronic hematoma Myositis ossificans
	Related to fascia	Chronic exertional compartment syndrome (CECS) Muscle hernia

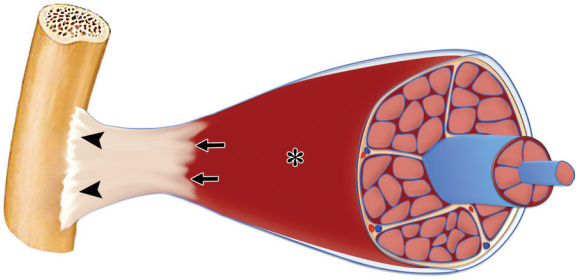

Figure 1. Diagram of the muscle-tendon-bone unit. Skeletal muscle (*) powers the unit, shortening and lengthening to initiate and control movement. Muscle fibers interdigitate with the free tendon at the MTJ (arrows). The tendon attaches to the bone at the enthesis (arrowheads). A collagen framework (blue) covers the muscle fibers, fascicles, and muscle itself.

Muscle Contraction

Muscle drives the muscle-tendon-bone unit through contractions that alter its length, resulting in motion of the tendon and bone and thus the limb. At the microscopic level, cross-linking between actin and myosin filaments within sarcomeres residing in muscle fibers initiates a chain of forces resulting in fiber lengthening or shortening (11).

There are three types of contraction, depending on how muscle fiber length is altered as it encounters a resistive load (11,12). In concentric exercise, such as lifting a weight, the muscle shortens as its force exceeds the resistive load. In isometric exercise, the forces of contraction and resistive load are equal and there is no change in muscle length. In eccentric exercise, such as controlled lowering of a weight, muscle force is less than the resistive load and the muscle actively lengthens.

Compared with eccentric exercise, concentric and isometric exercise are associated with recruitment of more muscle units and higher energy expenditure, oxygen utilization, and lactate production (13). Transient mild increases in T2 signal intensity immediately after vigorous concentric exercise parallel known increases in water content with exertion; these resolve within minutes (14). Eccentric contractions generate force concentrations that are significantly greater than with concentric contractions (9,15). Moreover, intense eccentric exercise, even in the absence of any discrete injury, can result in prolonged muscle signal intensity alterations.

Muscle Power

A muscle's capacity to generate movement relies on its power, which is determined by its functional capacity for contraction as well as its anatomy and architecture. A muscle's power depends on a host of factors, which include the following: *(a)* the composition, size, and length of its fibers; *(b)* the muscle's size, length, and moment arm; and *(c)* most important, the precise arrangement by which a muscle's fibers interface with its tendon.

The dominant skeletal muscle fiber types are type 1 (slow twitch) and type 2 (fast twitch). Type 1 fibers exhibit lower power but contain more mitochondria and myoglobin, affording tremendous capacity for repetitive and extended periods of contraction (11). Type 2 fibers display higher power for short bursts of activity owing to a greater number of glycolytic enzymes but cannot function for long durations and have a lower threshold for injury (11,16). Regardless of fiber type, longer fibers exhibit a greater capacity to shorten and lengthen. A larger number of fibers generates a stronger contraction force; hence, contraction power is proportionate to muscle size (9).

A muscle's moment arm is defined as its effectiveness in generating movement over a distance. This is determined by the muscle's length, its attachment angle to the bone, the position and range of motion of the bone/joint being moved, and the number of joints crossed by the muscle. A muscle with a long moment arm needs to

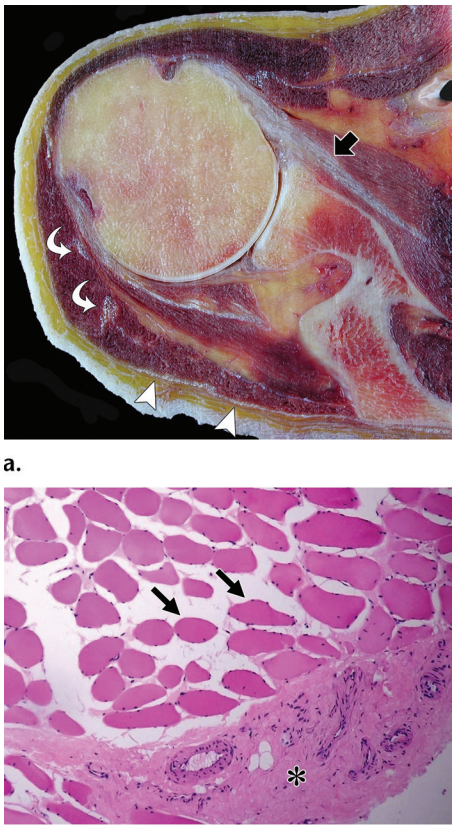

a.

b.

Figure 2. Collagen framework of muscle. **(a)** Anatomic cross section in the axial plane through the right shoulder shows the collagenous tendon of the subscapularis within the muscle belly (black arrow). Fine collagenous tendon fibers are seen interspersed within the deltoid muscle (white arrows), forming its fibrous framework. The collagenous epimysium covering the muscle is well visualized as a silvery band on the surface of the posterior deltoid muscle (arrowheads). (Courtesy of Donald Resnick, MD, University of California, San Diego, Calif.) **(b)** Photomicrograph of histologic specimen shows the epimysium (*) at the muscle surface. Individual muscle fibers are seen in cross section with their characteristic eccentric nuclei (arrows). (Hematoxylin-eosin stain; original magnification, ×200.) (Courtesy of Gabriel Varela, MD, Hospital Pablo Tobón Uribe, Medellín, Colombia.)

Figure 3. Bilateral traumatic tears of the hamstring tendons at their ischial origins in a 46-year-old former track athlete who slipped on wet grass. Large-field-of-view coronal T2-weighted fat-suppressed MR image of the pelvis shows bilateral avulsions of the hamstring tendons from the ischium. On the right, there is considerable proximal retraction of the semimembranosus and conjoint tendons (straight arrows) with surrounding edema/hemorrhage. The underlying tendons are thickened and irregular, related to degenerative tendinosis. On the left, there is also a complete tear of the hamstring tendons (curved arrow), but there is only mild proximal retraction of the torn tendon ends and less pronounced underlying tendinosis and adjacent edema.

generate more force to produce the same angular displacement as one with a shorter moment arm (9,12). Long muscles, particularly those that cross two articulations, have longer moment arms and therefore generate more force (16).

Muscle power is greatly influenced by architectural organization, with the highest forces generated by muscles that have muscle fibers inserting on the tendon at an angle (12,17). It is the long powerful pennate muscles of the lower extremity, particularly those that cross two joints and have a high proportion of type 2 fibers, that are at highest risk for muscle strain.

Indirect Injury

Muscle Strain

Strain is an acute indirect muscle injury that occurs during activity, typically related to excessive stretching of a contracted muscle during eccentric exercise while engaged in sports that emphasize speed and power, such as soccer, American football, rugby, and track and field (18). Some authors prefer the term *tear* rather than *strain* for such injuries, noting that *strain* is often applied indiscriminately to a range of muscle injuries that vary in etiology and pathophysiology (2). Strain is the most common injury resulting in lost playing time in professional athletes, sidelining over one-third of soccer and football players during a typical season (2,19).

Strains have traditionally been divided into three grades based on clinical severity. Grade 1 is a mild injury resulting in pain without loss of range of motion and function, so that the athlete is able to continue activity soon after the injury. Grade 2 is a moderate injury with loss of muscle strength and range of motion. Grade 3 is a severe injury, typically related to a complete tear, with loss of function (20,21). Grading of muscle

Figure 4. Avulsion fracture of the anterior superior iliac spine after a skating injury in a skeletally immature adolescent boy. **(a)** Anteroposterior radiograph of the left hip shows a subtle thin, curvilinear avulsed bone fragment (arrowheads) below the anterior superior iliac spine. **(b)** Sagittal T2-weighted fat-suppressed MR image of the hip shows complete avulsion of the sartorius tendon (arrows), as well as the adjacent tensor fascia lata and gluteus medius fascia (arrowheads). The avulsed tissues are displaced inferiorly from the iliac brim, with fluid filling the gap (*). Note the intramuscular edema/hemorrhage in the gluteus medius muscle dissecting along the course of its muscle fibers. The bone fragment is difficult to appreciate at MR imaging, blending imperceptibly with the low-signal-intensity tendon.

a. **b.**

Figure 5. Gastrocnemius strain injury in a 33-year-old man. Coronal **(a)** and axial **(b)** proton-density–weighted fat-suppressed MR images of the left calf show a moderate-grade MTJ strain of the lateral gastrocnemius (black arrows in **a**) and a low-grade strain at the distal MTJ of the medial gastrocnemius (white arrow). The myotendinous injury of the lateral gastrocnemius shows irregularity of the tendon with edema in the adjacent muscle and tracking along the fascicles, resulting in a feathery pattern. Note the thin layer of fluid on the surface at the distal tip of the medial gastrocnemius overlying its superficial tendon.

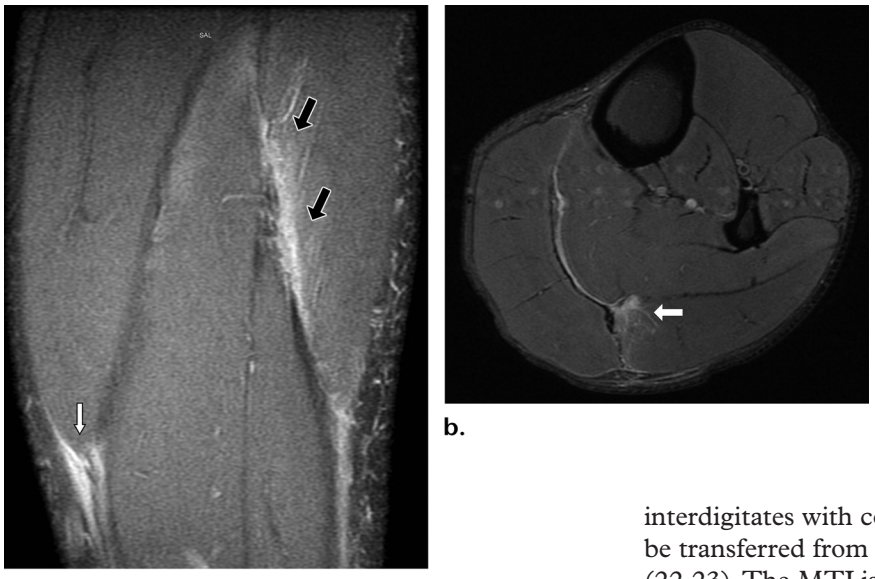

b.

a.

injury is evolving and is discussed further at the end of this article.

Myotendinous Junction.—The majority of strain injuries take place at the MTJ, where muscle interdigitates with collagen, allowing force to be transferred from the muscle to the tendon (22,23). The MTJ is a specialized region where fingerlike processes from the muscle increase the muscle's contact surface area with the tendon by 10-fold, dissipating energy over a larger area, thereby decreasing focal stress accumulation (24). Despite its specialized anatomy, the MTJ exhibits less capacity for energy absorption than muscle and tendon (16). In animal models, the

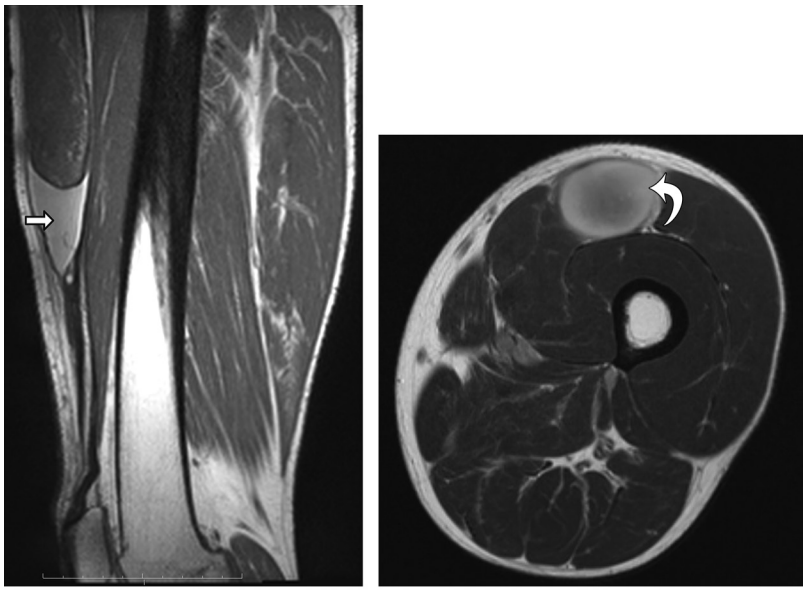

a. b.

Figure 6. Complete tear of the rectus femoris at the MTJ in a 45-year-old male soccer player. **(a)** Sagittal proton-density–weighted MR image of the left thigh shows a complete tear of the distal MTJ of the rectus femoris muscle, with a fluid-filled gap (arrow) between the retracted muscle and the distal free tendon. **(b)** Axial T1-weighted MR image obtained through this gap shows high signal intensity (arrow) related to subacute hemorrhage replacing the torn tissues.

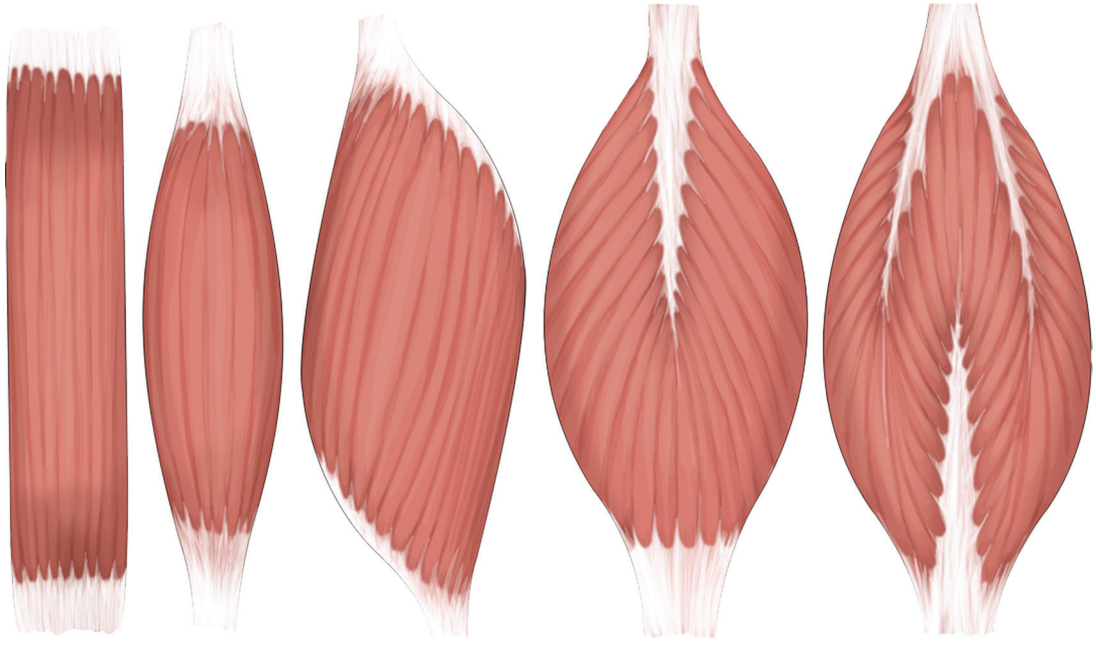

a. b. c. d. e.

Figure 7. Muscle architecture, or the physical arrangement of muscle fibers, affects the muscle's ability to produce movement and generate force. **(a, b)** The fibers of parallel muscles run along the long axis of the muscle and can be either strap **(a)** or fusiform **(b)** in configuration. Strap muscles have less prominent but broadly attaching tendons, while fusiform muscles have tapering tendons at both ends. The tapering at the end of a fusiform muscle results in a smaller area of concentrated force. **(c–e)** Pennate muscles have one or more tendons inserting into and extending most of the length of the muscle, with muscle fibers inserting onto the tendon at an angle along a long length of the tendon. The tendon, and therefore the MTJ, is located peripherally in a unipennate muscle **(c)** and centrally in a bipennate muscle **(d)**. **(e)** A multipennate muscle exhibits multiple discrete tendons, and injuries may be limited to portions of the muscle around one of its muscle-tendon units. (Courtesy of Aaron Lemieux, MD, University of California, San Diego, Calif.)

Figure 8. Complete tear of the biceps tendon in a 54-year-old man. Sagittal T2-weighted fat-suppressed MR image of the elbow shows a complete tear of the long head of the biceps tendon. Proximal retraction of the muscle and torn tendon (arrows) is related to the biceps muscle's parallel architecture, which allows a large range of excursion and shortening. This degree of retraction implies concomitant injury to the lacertus fibrosus, which normally constrains proximal migration of the tendon.

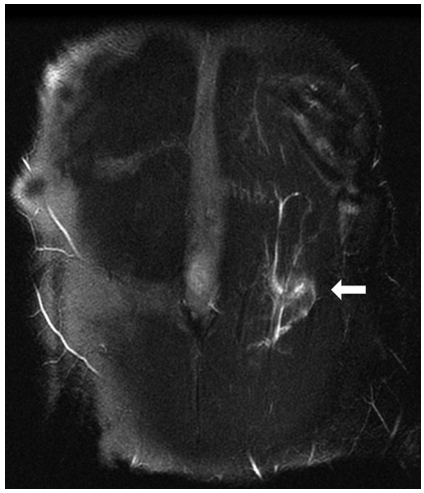

Figure 9. Acute muscle strain of the rectus abdominis in a 31-year-old man. The injury occurred while the patient was playing tennis. Coronal T2-weighted fat-suppressed MR image of the anterior abdominal wall shows edema within the left rectus abdominis muscle (arrow) related to strain injury.

average tension leading to MTJ failure is only 20% greater than the maximum isometric tension normally generated during activity (24).

The MTJ is located at a variable distance from the bone, and the tendinous portion located between the bone and the MTJ is referred to as the "free tendon" (25). Muscles with short free tendons, such as the gluteus maximus and deltoid, appear to insert virtually directly on the bone, whereas muscles such as the rectus femoris, biceps brachii, and plantaris have free tendons several centimeters in length (Fig 6).

Muscle Architecture.—There is considerable variation in muscle architecture, altering the precise location and configuration of the MTJ, which are fundamental to understanding the variable MR imaging and US findings related to strain injury. Muscles are organized in either a parallel or pennate fashion (Fig 7). In parallel muscles, the fibers and fascicles are oriented parallel to the tendon and insert on the tendon at the end of the muscle via a short discrete musculotendinous zone. Parallel muscles exhibit larger ranges of excursion but produce relatively little force and thus are uncommonly strained (15).

Fusiform parallel muscles such as the biceps brachii have tendons at either end, resulting in a spindle-shaped appearance. Strap parallel muscles such as the pronator quadratus and sartorius have less conspicuous tendons, giving rise to a band-like configuration. Injury to parallel muscles typically takes place within the tendon, often resulting in significant muscle shortening and retraction (Fig 8). The rectus abdominis is a strap muscle, but it is subdivided by rigid transverse fibrous bands that restrict its motion, resulting in a higher risk of strain during stretching and twisting than for other parallel muscles (26) (Fig 9).

In pennate muscles, muscle fibers insert on the tendon at an angle, termed the *pennation angle*. The interdigitation between muscle and tendon fibers typically takes place over several centimeters, either within or on the surface of the muscle, so the MTJ is not discrete, as it is in parallel muscles; rather, it is a long transition zone (27). Oblique attachment relative to the line of tendon traction results in a greater surface area for insertion, allowing packing of more fibers per volume, giving rise to greater force. However, a portion of the contraction force transmitted to the tendon is dampened by the fiber obliquity and transferred to drawing the tendon and epimysium closer together, mitigating the change in muscle volume during contraction (9,17).

Pennate muscles have shorter fibers and are less capable of excursion, increasing their risk for strain during stretching. Additionally, muscle fibers with steeper pennation angles (ie, more perpendicular to the tendon) are at highest risk for strain (11).

Unipennate muscles have a peripheral tendon that is continuous with the epimysium, forming a superficial MTJ with muscle fibers inserting

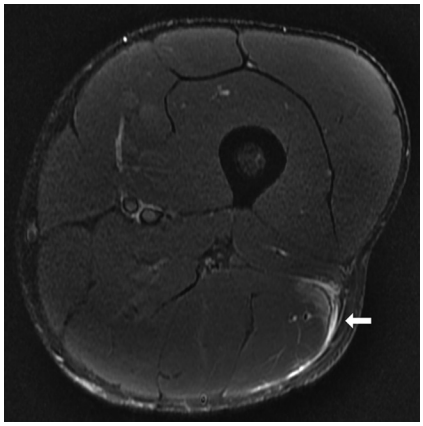

Figure 10. Low-grade sprain of the long head of the biceps femoris in a 27-year-old male professional athlete after a game. Axial T2-weighted fat-suppressed MR image of the left thigh shows mild muscle edema related to a low-grade MTJ injury of the distal biceps femoris adjacent to its superficial aponeurotic tendon, with surrounding fluid overlying the epimysium (arrow).

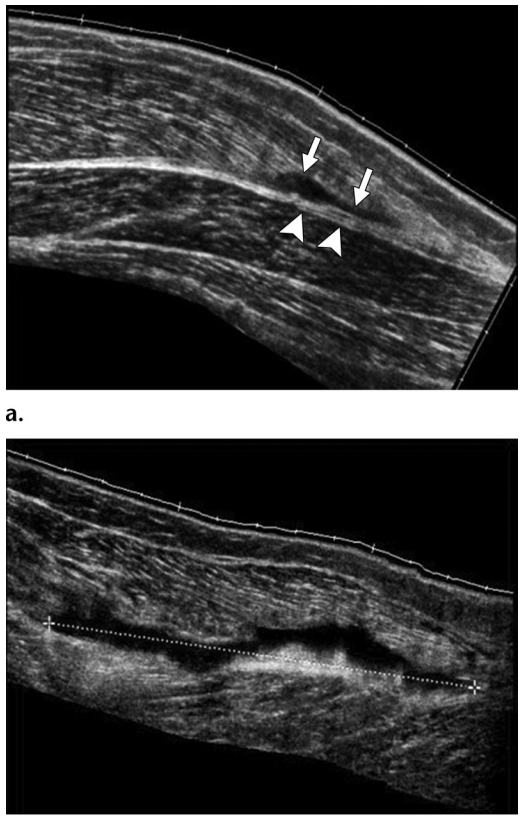

a.

b.

Figure 11. **(a)** Aponeurotic distraction injury of the medial head of the gastrocnemius in a 33-year-old male soccer player with acute onset of pain while playing. Longitudinal gray-scale US image of the calf shows a hypoechoic region (arrows) within the distal deep muscle fibers of the medial head of the gastrocnemius, which are separated from the echogenic superficial aponeurotic tendon on its deep surface (arrowheads). Note the pennate architecture of the gastrocnemius muscle, with its fibers inserting at an angle along the length of the higher-signal-intensity collagenous tendon. **(b)** More extensive injury in a 25-year-old male soccer goalkeeper injured during play. Longitudinal gray-scale US image of the calf shows an elongated fluid collection at the MTJ (between cursors) with irregularity and waviness of the muscle fibers. There is hyperechogenicity of the injured muscle with crimping and irregularity of the tendon, indicating that it is also damaged.

on it from one side. The tendon may be focal and band-like or a broad sheet-like aponeurosis. Unipennate strain most commonly affects the powerful hamstring muscles: the biceps femoris of the hamstring complex is the most frequently strained muscle in the human body, followed by the rectus femoris and gastrocnemius muscles (Fig 10) (1,2,25,27,28). Long unipennate muscles often have tendons at both ends of the muscle, with the proximal and distal tendons located on opposing surfaces, reversing the typical side of injury along its length from proximal to distal. In unipennate muscles, strain injury typically abuts the muscle surface and is often associated with fluid accumulation superficial to the epimysium, even after low-grade injury.

It has been suggested that differential contraction of two adjacent muscle bellies that converge on a common tendon formed by the blending of their aponeuroses predisposes them to strain injury (aponeurotic distraction injury) (29,30). This pattern of injury is common at the distal gastrocnemius and soleus as their aponeuroses converge to form the Achilles tendon (27) (Fig 11). Tennis leg injuries of the calf involving these muscles demonstrate fluid accumulation in up to 50% of cases, characteristically between the unipennate gastrocnemius and soleus, whose aponeuroses lack adherence proximally due to the presence of an interposed plantaris tendon (31) (Fig 12). A prominent amount of fluid in such injuries can lead to overgrading of unipennate strain, as it is often disproportionate to the degree of underlying tissue damage.

In bipennate muscles, the tendon is located within the muscle and the muscle fibers insert onto the tendon from both sides. Because the MTJ is central, strains results in a feathery pattern of intramuscular edema with a relative paucity of superficial fluid, unless the injury is high grade (Fig 13). The term *multipennate* is imprecise, as it is applied to muscles that insert via multiple discrete tendons, regardless of whether the muscle fibers attaching to these tendons are parallel or pennate. Injuries of multipennate muscles like the deltoid, subscapularis, infraspinatus, and pectoralis major produce highly variable patterns of injury, depending on which segments are injured. Segmental injuries are commonly seen at the pectoralis, typically related to disproportionate tearing of its sternal portion (32) (Fig 14).

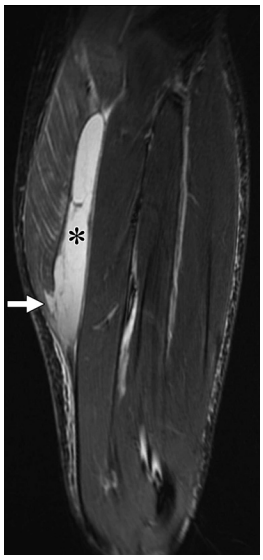

Figure 12. Fluid accumulation disproportionate to the degree of myotendinous damage in a 49-year-old man with a tennis leg injury. Coronal T2-weighted fat-suppressed MR image of the left calf shows a moderate-grade strain of the distal end of the medial head of the gastrocnemius (arrow), with a large fluid collection (*) between the gastrocnemius and soleus. The potential space between these muscles can accumulate large amounts of fluid even in low-grade strain. The plantaris tendon that normally resides in this location is not visualized due to a high-grade tear.

Figure 13. MTJ strain of the supraspinatus in a 30-year-old man with acute onset of shoulder pain while lifting weights. Axial T2-weighted fat-suppressed MR image of the right shoulder shows muscle edema on both sides of the centrally located supraspinatus tendon (arrows) related to a low-grade MTJ strain. Note the oblique orientation of the muscle fibers approaching the central tendon, typical of a bipennate muscle.

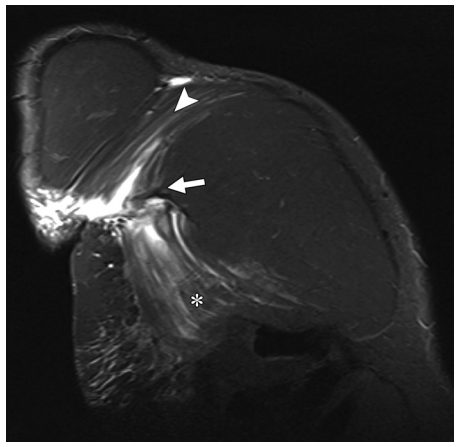

Figure 14. Tendon tear of the sternal head of the pectoralis in a man with acute right chest pain and swelling after bench-pressing a 400-lb (180-kg) weight. Oblique coronal T2-weighted fat-suppressed MR image of the pectoralis shows a complete tear of the tendon involving the sternal head of the pectoralis (arrow). There is considerable muscle edema in the abdominal head (*) related to the tendon tear. Milder edema is evident in the superior clavicular head (arrowhead), where the tendon remains intact.

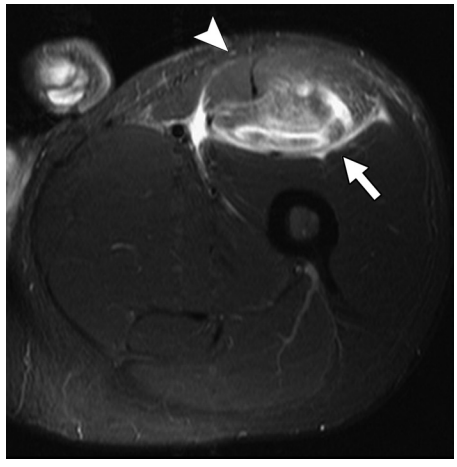

Figure 15. Strain of the direct head of the rectus femoris muscle in a man. Axial T2-weighted fat-suppressed MR image of the left thigh shows a moderate-grade injury of the muscle belly of the rectus femoris continuous with the direct head. There is epimysial fluid along the flat posterior aponeurosis (arrow), which arises from the distal two-thirds of the muscle before merging distally with the vastus tendons to form the quadriceps tendon. The portion of the muscle derived from the indirect head containing its central tendon (arrowhead) is not involved.

The rectus femoris exhibits unique anatomy, with a unipennate peripheral component derived from its direct head that encloses a central bipennate muscle derived from its indirect head, effectively a muscle-within-muscle configuration. The proximal muscle has a superficial anterior aponeurosis, whereas the distal muscle has a posteriorly located aponeurosis that arises from the knee (33). This complex arrangement leads to a variety of injury patterns involving the superficial aponeuroses, the peripheral unipennate muscle, and/or the central bipennate muscle. The bulk of the muscle belly is continuous with the direct head and is located posterolaterally (Fig 15). Selective injury of the central bipennate muscle leads to a bull's-eye appearance of central edema after a partial tear or a degloving pattern with a central void related to a complete tear with retraction of the indirect head component (34) (Fig 16).

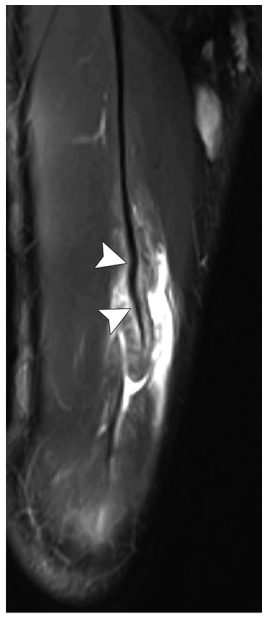

a.

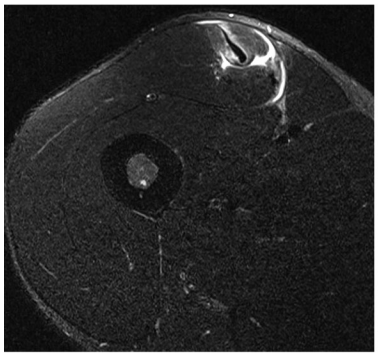

b.

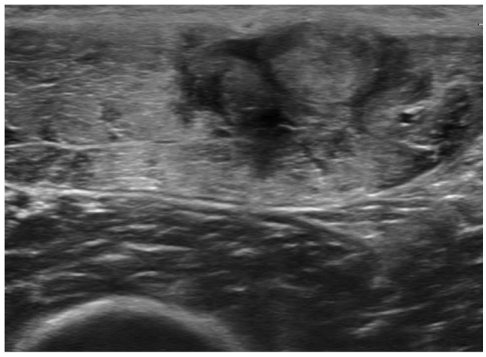

c.

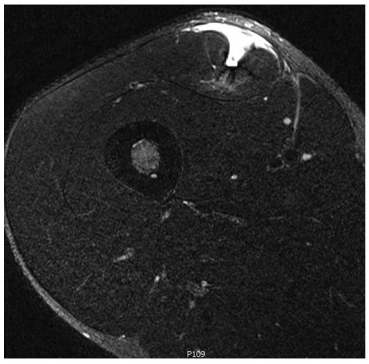

d.

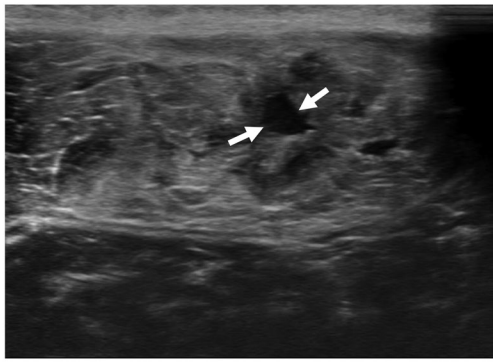

e.

Figure 16. Tear of the central tendon of the indirect head of the rectus femoris in a 16-year-old male soccer player with acute onset of right thigh pain while kicking a soccer ball. He had a palpable defect at the anterior midthigh. **(a)** Coronal proton-density–weighted fat-suppressed MR image of the right thigh shows undulation of the central tendon of the indirect head of the rectus femoris (arrowheads), with fluid surrounding its inferior margin and edema in the adjacent musculature. **(b, c)** Axial proton-density–weighted fat-suppressed MR **(b)** and transverse gray-scale US **(c)** images at the midthigh show edema/hemorrhage within the muscle and fluid surrounding the central indirect head of the rectus femoris. Note the increased echogenicity and lobulation of the centrally located indirect head on the US image. **(d, e)** Axial proton-density–weighted fat-suppressed MR **(d)** and transverse gray-scale US **(e)** images at a more inferior level show a fluid-filled gap (arrows in **e**) related to tearing of the distal end of the tendon, with lack of visualization of the tendon.

Delayed-Onset Muscle Soreness

Delayed-onset muscle soreness (DOMS) is a stretching injury caused by unaccustomed, prolonged, or overly vigorous eccentric exercise. The intensity, rather than the duration, of exercise is most closely related to the risk of developing DOMS (35). While strain injuries develop acutely during activity, patients with DOMS report gradual onset of muscle pain, stiffness, and swelling several hours or days after activity, followed by spontaneous resolution within 1–2 weeks (36). The etiology of DOMS is related to increases in compartment pressure and water content that disproportionately affect type 2 fast-twitch fibers, with disruption of the Z bands of sarcomeres throughout the muscle (37). Diffusion tensor imaging is particularly sensitive for noninvasive identification of these microstructural alterations (38). Inflammation and necrosis are not consistent or dominant features (39).

At routine MR imaging, muscle enlargement and increase in fluid signal intensity on

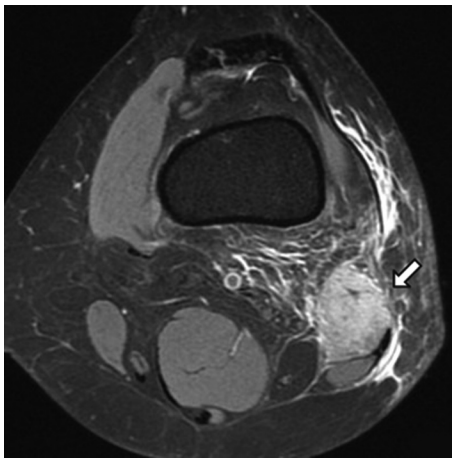

Figure 17. DOMS in a 15-year-old boy after prolonged vigorous use of a twist board 2 days earlier. Axial T2-weighted fat-suppressed MR image through the left distal thigh shows uniform muscle edema isolated to the short head of the biceps femoris (arrow), associated with edema at the surface of the muscle, overlying fascia, and subcutaneous tissues. Note the uniform muscle involvement, without localization to the MTJ as would be expected in muscle strain. (Courtesy of Enrique Bosch, MD, Clinica Alemana, Santiago, Chile.)

a. **b.**

Figure 18. Contusion caused by direct impact with a striking object. **(a)** Diagram shows a contusion injury to the quadriceps musculature. **(b)** Contusion injury in a 22-year-old man with a history of a direct blow to the thigh 4 weeks earlier. Sagittal T2-weighted fat-suppressed MR image of the left thigh shows a poorly marginated heterogeneous mass-like lesion within the vastus intermedius muscle (arrow) overlying the anterior surface of the femur, related to a contusion injury with hematoma and surrounding edema. Impact when muscle is relaxed results in deep muscle damage adjacent to the bone surface, where force concentration is maximal.

T2-weighted images with preservation of muscle architecture reflect the increased intramuscular and interstitial fluid seen throughout the damaged muscle at histologic analysis (39) (Fig 17). Signal intensity alterations affect either a single muscle or a small group of functionally similar muscles, without the MTJ localization typical of muscle strain or any architectural distortion. MR imaging findings peak 3–5 days after injury, but subtle residual alterations can persist for up to 80 days (36).

Direct Trauma

Contusion

Contusion is an acute injury caused by a direct nonpenetrating blow to the muscle, typically affecting the anterior thigh, posterior thigh, or anterolateral upper arm (Fig 18). Contusion is second only to strain as a cause of lost playing time in the professional athlete. Injury severity is determined by the force of impact, size of the striking object, and the muscle's state of contraction. Small objects produce more damage than a large or flat object, as the impaction force is focal rather than distributed over a broader extent of tissues, explaining why athletic protective padding is designed to dissipate impact forces over a large area to minimize injury (40). Muscle damage results from compression of muscle by the striking object and compression of muscle between the object and underlying bone (2,19,23,30).

In professional contact athletes, the most commonly injured muscles are the rectus femoris and vastus intermedius at the anterior thigh (Fig 19). Nonathletes typically sustain contusions related to a blow or fall or being thrown from a vehicle. Such contusions show a wider anatomic distribution.

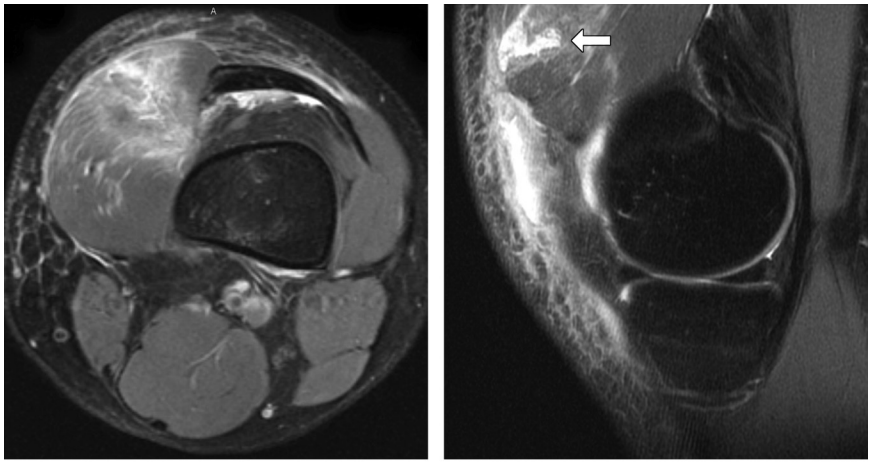

Figure 19. Contusion injury of the vastus medialis in an American football player who suffered a direct blow to the distal quadriceps muscle. **(a)** Axial proton-density–weighted fat-suppressed MR image of the left knee shows extensive edema in the vastus medialis muscle with overlying subcutaneous edema in the anteromedial knee at the site of impact, related to a muscle contusion. **(b)** Sagittal T2-weighted fat-suppressed MR image shows muscle tissue disruption (arrow) with intramuscular fluid within the muscle belly. Unlike muscle strain, contusion injury does not localize to the MTJ or epimysium.

Figure 20. Acute hematoma within the vastus medialis in a male American football player who was struck in the thigh by a helmet. Axial proton-density–weighted fat-suppressed MR image of the left knee 6 hours after injury shows an acute low-signal-intensity hematoma (arrows) within the vastus medialis muscle, surrounded by a halo of muscle edema. There is diffuse subcutaneous edema; the underlying bone appears normal.

Figure 21. Subacute hematoma in a 48-year-old man with a persistent mass after a fall from a bicycle several months earlier. Coronal T1-weighted MR image of the left hip shows a subacute hematoma at the interface of the fascia and subcutaneous fat adjacent to the greater trochanter, typical of a Morel-Lavallée lesion. The heterogeneity of the mass reflects blood in various stages of degradation, with methemoglobin seen in the inferior portion of the lesion (arrow). The low-signal-intensity rim in such lesions (arrowheads) often relates to entrapment of hemorrhage between the deep and superficial layers of the iliotibial fascia rather than hemosiderin deposition.

Contusion results in an admixture of focal intramuscular hematoma and interstitial hemorrhage dissecting through the loosely organized muscle parenchyma. There may be accompanying injury to the subcutaneous tissues, fascia, and/or bone (18,41). While contusions often appear larger than strain injuries, fiber disruption is primarily limited to muscle, which heals faster than tendon, so the recovery time after contusions tends to be shorter than that after strains (2,28). In one large study evaluating thigh injuries in professional soccer players, contusions resulted in half the time lost to sport as compared with strains (41,42). Contusions are managed conservatively with cooling, elevation, compression bandaging, and aggressive rehabilitation (41). The utility of hematoma aspiration, injection with steroids or platelet-rich plasma, and surgery for such injuries remains controversial (4).

Intracompartmental Hemorrhage.—Intramuscular hematoma is easily recognized owing to local architectural distortion, appearing as an intramuscular mass of variable signal intensity depending on the stage of blood degradation. The evolution of blood degradation within intracranial hematoma at MR imaging is well described; muscle fol-

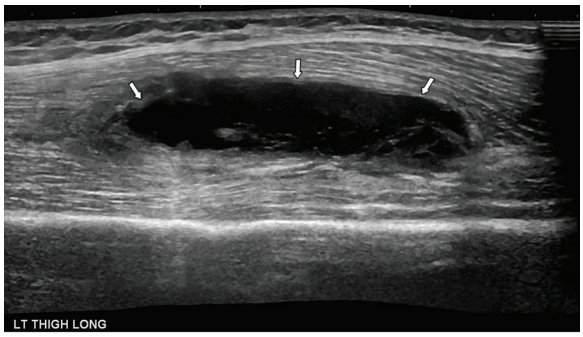

a.

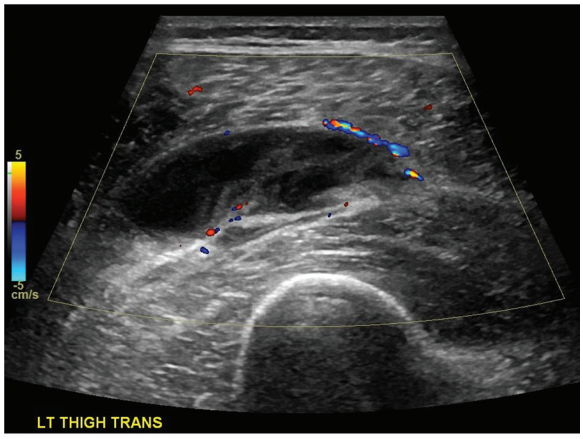

b.

Figure 22. Large left thigh hematoma in a 53-year-old man who was struck by a car while riding a bicycle. **(a)** Longitudinal gray-scale US image shows a large predominantly anechoic fluid collection within the vastus lateralis muscle (arrows) with a small amount of internal debris, consistent with a subacute hematoma. **(b)** Transverse color Doppler image confirms that the collection is avascular, as expected for a hematoma.

lows the same pattern, albeit with a more variable time course (43). Acute hematoma exhibits low T1 and T2 signal intensity related to intracellular deoxyhemoglobin (Fig 20). In the early subacute phase, deoxyhemoglobin converts to intracellular methemoglobin, increasing T1 signal intensity (Fig 21). In the late subacute phase, as red cells lyse and methemoglobin becomes extracellular, T2 signal intensity also increases. The final degradation products are hemosiderin and ferritin, closely related substances responsible for the low signal intensity of chronic hemorrhage.

At US, intramuscular hematoma is a key finding in significant muscle tear. Acute hemorrhage immediately after injury produces an amorphous ill-defined region of hyperechogenicity that is easily overlooked, particularly when associated aponeurotic injury allows blood to escape via the muscle's surface wrappers (44). Over a period of a few hours, the hemorrhage evolves into an anechoic fluid collection, which then converts over a period of a few days into a hypoechoic fluid collection that may contain fluid-fluid levels, septa, and/or internal debris (29,30) (Fig 22). The resolution

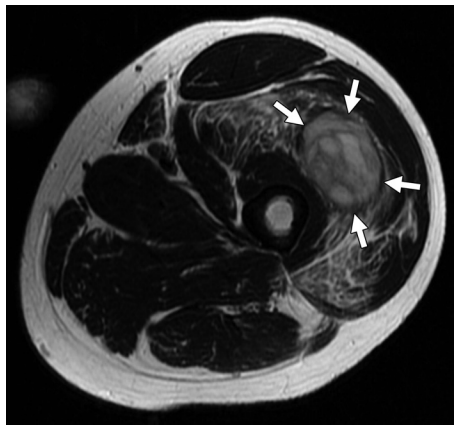

Figure 23. Subacute hematoma in the vastus intermedius in a 27-year-old soccer player who sustained a direct blow to the thigh 2–3 weeks earlier with persistent pain. Axial T2-weighted MR image of the left midthigh shows a large subacute hematoma (arrows) in the vastus intermedius muscle adjacent to the femur, surrounded by ill-defined parenchymal bleeding dissecting through the adjacent muscle tissue in a feathery pattern that mirrors the muscle's interstitial planes.

of the hematoma takes place over a period of days to weeks, depending on the size of the lesion.

Interstitial Hemorrhage.—Unlike brain hemorrhage, muscle hemorrhage often includes a large poorly marginated interstitial component that may degrade at an even more variable rate than focal muscle hematoma (45,46). Interstitial bleeding can be substantial enough to lead to circulatory compromise, particularly in large muscles or if associated with fascial injury that can decompress the compartment, allowing unrestricted bleeding (47). Interstitial hemorrhage results in increased girth and poorly marginated hemorrhage dissecting in the muscle, which can be mistaken for fat on T1-weighted images if it contains substantial methemoglobin, leading to underestimation of the amount of blood in the muscle parenchyma (48) (Fig 23).

Differential Diagnosis.—Necrotic primary neoplasms and hemorrhagic muscle metastases can contain substantial blood products and fluid-fluid levels, simulating a traumatic hematoma (49). Hematoma formation without a clear history of trauma or recurring hemorrhage at the same site should raise concern for an underlying lesion such as a neoplasm, vascular malformation, or pseudoaneurysm. In malignancies, methemoglobin is maximal in regions of tumor necrosis, typically located centrally as the tumor outstrips its blood supply (Fig 24).

In contradistinction, it is the periphery of an early subacute hematoma that generally converts

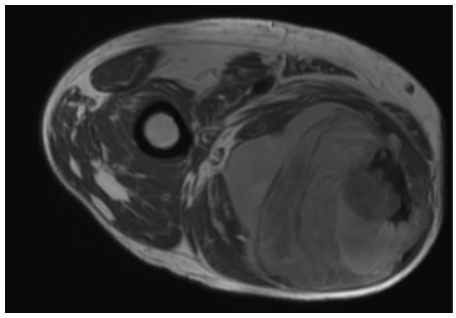

Figure 24. Subacute intralesional hemorrhage in a right thigh sarcoma in a 63-year-old man after radiation therapy–induced tumor necrosis. Axial T1-weighted MR image of the right thigh shows hyperintense signal reflecting methemoglobin in a large hemorrhagic mass in the posterior compartment of the thigh. Significant internal bleeding can also be seen in other necrotic primary tumors as well as in intramuscular metastases related to renal cell carcinoma, thyroid carcinoma, and other hypervascular malignancies.

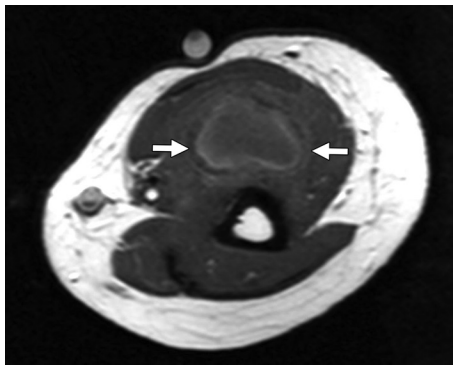

Figure 25. Subacute hematoma in a 31-year-old woman with a history of an upper arm mass after direct trauma. Axial T1-weighted MR image through the left upper arm shows a subacute hematoma in the brachialis muscle. The hematoma has a high-signal-intensity rim (arrows) related to peripheral methemoglobin formation, typical of an early subacute hematoma.

to methemoglobin most rapidly, forming a hyperintense rim at the edges of the hematoma (50) (Fig 25). There can be significant overlap in the appearance of hemorrhagic neoplasm and hematoma; US is recommended for serial follow-up of any equivocal hematomas to ensure resolution.

Laceration

Muscle laceration results from acute direct penetrating trauma by a sharp object, typically a pointed item such as a knife. Such injuries disrupt the skin, subcutaneous tissues, and fascia before piercing the muscle. MR imaging demonstrates a clearly demarcated linear defect in the muscle filled with blood and fluid, associated with skin disruption, subcutaneous edema, and soft-tissue gas (Fig 26). Laceration can also result from an internal object such as the sharp end of a fractured bone; in such cases, the overlying soft tissues may not be injured (51). Ballistic injuries and therapeutic injections are not considered lacerations.

The injury is evident clinically, so the role of imaging in muscle laceration is limited to select cases for evaluation of the extent of tissue damage and identification of complications such as neurovascular damage, retained foreign bodies, and secondary infection (52). Lacerations are typically managed conservatively. If necessary, surgical repair of muscle is performed for restoration of function but has a high failure rate, as sutures pull out of muscle more readily than from structured tissues like tendons (53,54).

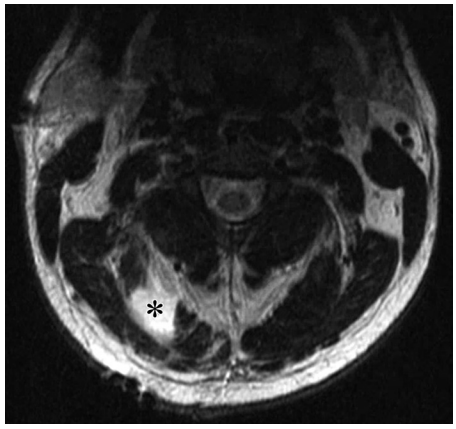

Figure 26. Stab wound to the neck in a 30-year-old man. Axial T2-weighted MR image shows a large fluid-filled void in the posterior right paraspinal muscles (*) with sharply marginated linear edges, characteristic of a penetrating injury. Injury of the overlying trapezius muscle was present on an adjacent image (not shown) related to angulation of the knife. The skin was closed and stapled before imaging.

Disorders of the Connective Tissues

Disorders related primarily to the connective tissue fascia that organizes muscles into compartments form part of the broad spectrum of muscle injury. The upper and lower arm are each divided into anterior and posterior compartments; the thigh is separated into anterior, posterior, and medial compartments; and the calf is divided into anterior, lateral, deep posterior, and superficial posterior compartments (Fig 27). The fascia surrounding each compartment restricts the ability of its contents to expand. Expansion within a confined space increases compartment pressure, resulting in altered pressure gradients between the compartment and the vasculature, compromising capillary and neural microcirculation, venous outflow, and ultimately arterial inflow, which results in hypoxia, acidosis, and altered cell permeability (55).

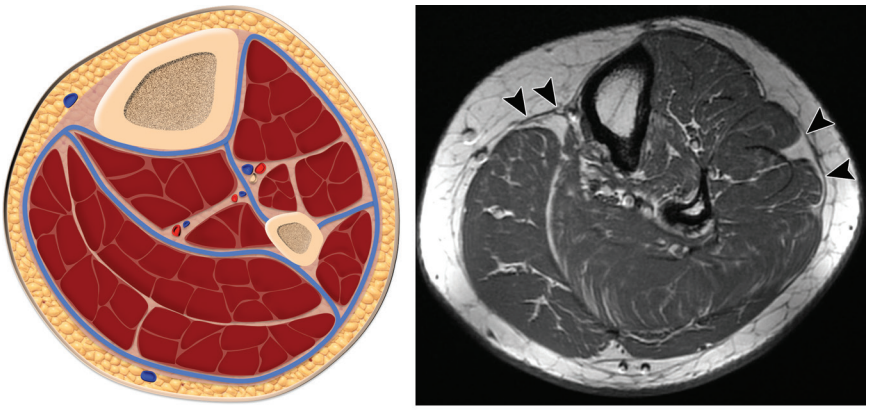

a. b.

Figure 27. Cross sections of the left lower leg illustrating compartment anatomy. **(a)** Diagram shows the location of the connective tissue fascia (blue lines) that separates the muscles of the calf into anterior, lateral, deep posterior, and superficial posterior compartments. **(b)** Corresponding axial T1-weighted MR image shows normal muscle with smooth convex outer margins and normal muscle architecture with interspersed high-signal-intensity fat and low-signal-intensity collagen. The low-signal-intensity connective tissue framework and its resultant organization of muscle tissue is most evident on axial T1-weighted images. The superficial fascia forming the compartments (arrowheads) is visible in this older patient due to mild muscle atrophy. It may not be clearly separable from the muscle aponeuroses in thin patients.

Untreated compartment syndrome can progress to muscle necrosis, resulting in muscle dissolution and its replacement by fat, fibrosis, or, less commonly, sheet-like or mass-like calcification (56). Systemically, myonecrosis can result in enough release of myoglobin to cause acute renal insufficiency or even death. Compartment syndrome has numerous causes including acute and repetitive trauma, recent surgery, prolonged pressure, thrombosis, and space-occupying lesions within the compartment; this review emphasizes only traumatic causes. Posttraumatic compartment syndrome may be acute or chronic, depending on its rate of onset and severity.

Acute Compartment Syndrome

Acute compartment syndrome is most commonly seen in the lower leg after a fracture; over 70% of cases of acute lower extremity compartment syndrome are the result of a tibial or fibular shaft fracture, often affecting multiple compartments simultaneously (55). While the anterior and lateral compartments of the calf are the most common sites of acute compartment syndrome, other locations such as the thigh, upper arm, forearm, and paraspinal musculature can also be affected. Patients classically present with the six classic signs of arterial insufficiency: pain disproportionate to the injury, paresthesia, pallor, paralysis, poikilothermia, and pulselessness (53,57).

MR imaging shows diffuse compartment bulging related to muscle enlargement and intracompartmental hemorrhage and/or fluid. T1-weighted signal intensity is normal or mildly increased due to interstitial hemorrhage, while T2-weighted images typically show slightly increased muscle signal intensity. Administration of intravenous contrast material emphasizes the altered muscle perfusion, demonstrating peripheral enhancement with central regions of hypoperfusion or frank liquefaction reflecting muscle necrosis (53,55) (Fig 28). Acute compartment syndrome is a surgical emergency requiring emergent fasciotomy, so imaging is rarely used, as it delays appropriate intervention.

Chronic Exertional Compartment Syndrome

Chronic exertional compartment syndrome (CECS) causes aching pain, cramping, and muscle tightness during exercise, typically of the anterior or lateral calf, and is often bilateral (58). Symptoms typically resolve rapidly after cessation of activity without structural damage, although rarely extreme cases can progress to acute compartment syndrome. Management consists of activity modification, with fasciotomy reserved for recalcitrant cases (59). The precise pathophysiology responsible for CECS remains unclear; proposed mechanisms include delayed egress of intracellular fluid from activated muscle fibers, metabolite-induced permeability alterations, and periosteal nerve irritation (60–62).

The clinical diagnosis of CECS is challenging, as periostitis, stress fracture, tendinopathy, functional popliteal artery compression, and nerve entrapment result in similar symptoms. CECS is diagnosed by invasively measuring compartment pressures before and after exercise. These

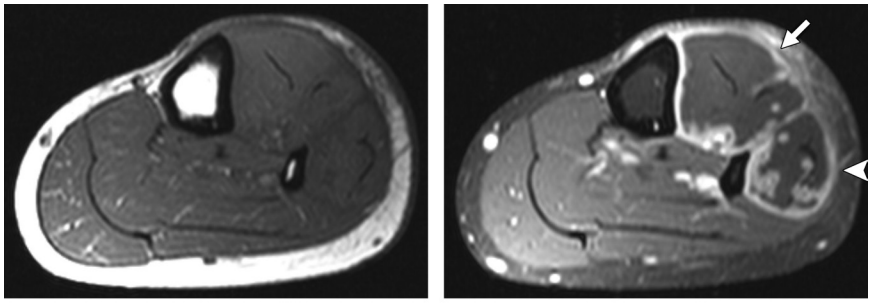

a. b.

Figure 28. Unrecognized compartment syndrome in a 33-year-old woman with foot drop and continuous pain after a fall 1 month earlier. **(a)** Axial T1-weighted MR image of the left calf shows mild bulging and minimal signal intensity increase in the anterior muscle compartment and effacement of intramuscular fat in the lateral compartment. **(b)** Axial T1-weighted fat-suppressed image after injection of intravenous contrast material shows disordered enhancement, with intense peripheral enhancement of the anterior (arrow) and lateral (arrowhead) compartments and large areas of central nonenhancement related to hypoperfusion and myonecrosis. The patient was treated with fasciotomy and débridement.

measurements are most accurate if obtained 1–5 minutes after exercise, as delayed measurements show considerable overlap between patients with CECS and asymptomatic controls (6,63). The value of pressure measurements has been questioned, given their lack of specificity and the wide variation in measured pressures related to technical factors such as catheter depth, limb position, and the muscle's contractile state.

Conventional MR imaging fluid-sensitive sequences performed immediately after exercise have shown high sensitivity for detecting transient signal intensity alterations noninvasively (60). Increased muscle signal intensity on fluid-sensitive images may be accompanied by muscle swelling and fascial edema; these alterations, identical to those after vigorous concentric contraction, are maximal immediately after exercise and resolve within 30 minutes (Fig 29). Quantitative T2 measurement, spectroscopy, and functional MR imaging afford even higher sensitivity (14,58,60,62). However, the specificity of imaging is not yet established. Andreisek et al (58) performed T2*-weighted and arterial spin labeling imaging after exercise and noted identical transient changes in asymptomatic volunteers and patients with CECS, although the latter group reported greater fatigue and pain.

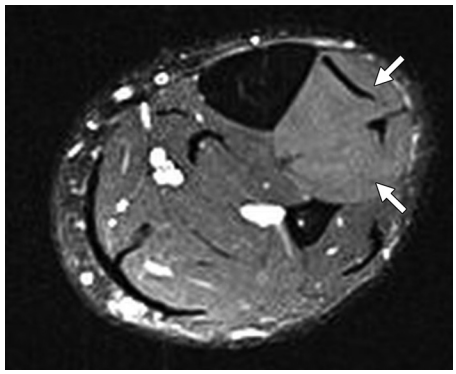

Figure 29. CECS in a 30-year-old man with transient left calf pain during running. Axial T2-weighted fat-suppressed MR image of the left calf immediately after 20 minutes of vigorous pedaling on an exercise bicycle shows bulging and mild signal intensity increase limited to the musculature of the anterior calf compartment (arrows). Pre-exercise MR images (not shown) were normal. (Courtesy of George Nomikos, MD, New York University, New York, NY.)

Muscle Hernia

Muscle hernias are the result of a fascial defect most commonly caused by a fracture, penetrating injury, or surgery, allowing muscle to protrude through the connective tissue (64). Less commonly, muscle hernia occurs at an intact but incompetent fascia thinned by injury, chronic compartment syndrome, or a congenital defect (typically located where the fascia is already attenuated by traversing vessels and/or nerves) (48,59). The most common location of muscle hernia is the anterior compartment of the calf, typically related to a medial defect allowing herniation of the tibialis anterior muscle. Other muscles prone to herniation include the extensor digitorum longus, peroneus brevis, peroneus longus, and gastrocnemius (64).

Muscle hernias are typically managed conservatively with support stockings. Repair of the fascial defect can result in acute compartment syndrome and is therefore rarely performed (65). In rare cases, herniated muscle may become incarcerated, necessitating urgent surgical intervention (66).

Patients with muscle hernia are typically young adults with a palpable mass that appears or enlarges during contraction, particularly in the upright position (65). While the diagnosis is often suspected clinically, imaging affords defini-

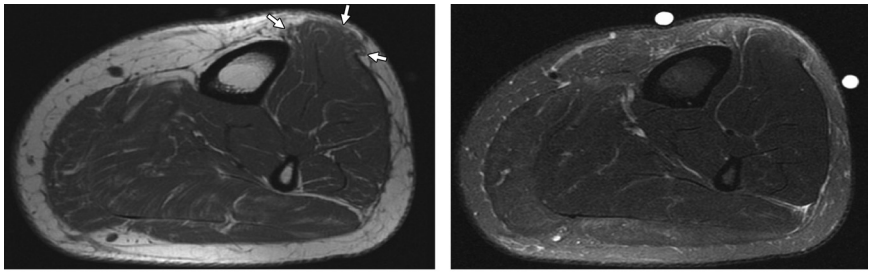

a. b.

Figure 30. Muscle hernia in a 32-year-old male runner with a palpable mass. The patient did not recall any injury. Axial T1-weighted **(a)** and T2-weighted fat-suppressed **(b)** MR images show bulging of the anterior tibialis muscle (arrows) through the superficial fascia adjacent to the tibia between the superficial markers bracketing the palpable mass. On the T1-weighted image, note that the muscle hernia shows signal intensity and feathery interdigitating fat and tendinous tissue typical of muscle architecture. Slight edema is seen in the muscle hernia and gastrocnemius muscle, likely related to overuse.

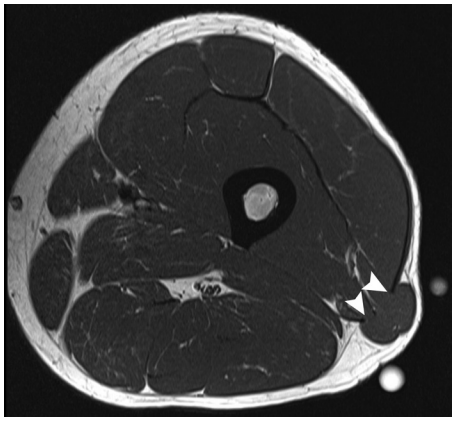

Figure 31. Posttraumatic muscle hernia in a man with a palpable mass. Axial T1-weighted MR image of the left thigh with superficial markers bracketing the palpable mass shows lobulated herniation of a portion of the vastus lateralis muscle (arrowheads) through a defect in the normal low-signal-intensity fascia.

tive diagnosis and patient reassurance. The MR imaging appearance of muscle hernia is distinctive, showing a protuberant or bulging mass with similar signal intensity and architecture as normal muscle (Fig 30). A fascial defect may be apparent if the hernia is large and there is adequate body fat outlining the fascial margins (64) (Fig 31).

MR imaging has limited sensitivity for small or transient hernias; US is more sensitive, as it allows dynamic imaging during contraction in the upright position (65) (Fig 32). At US, herniated muscle appears as a hypoechoic mass, typically less echogenic than normal muscle due to anisotropy, atrophy, or repetitive trauma; a defect in the normal hyperechoic fascia may also be visible (52).

Muscle Healing

Muscle exhibits considerable regenerative potential, so the majority of muscle injuries can be managed conservatively, generally with good functional outcomes. Muscle healing passes through similar overlapping stages regardless of whether the initial injury is caused by strain, contusion, or laceration. These include a brief destructive stage of hemorrhage and necrosis (0–2 days); an inflammatory stage of phagocytosis of necrotic tissue and angiogenesis (2–5 days); a repair stage of regeneration and revascularization (3–60 days); and a remodeling stage (3–60 days) of maturation of regenerating fibers, reintegration of newly formed tissue with native muscle and tendon, and organization of scar tissue (67,68). Satellite cells, the equivalent of stem cells in muscle, play a central role in this healing process (67).

Return to Play

In the athlete, allowing adequate healing before return to play is important to prevent reinjuring the weakened tissues. Reinjury is unfortunately common, occurring in up to 15% of strains, and generally requires a longer convalescence than after the initial trauma (69,70) (Fig 33). Functional recovery precedes full structural recovery, so residual imaging alterations may be present even after the athlete feels healed; whether such residua indicate a higher risk of reinjury is unclear (1).

Determining optimal rehabilitation time is imprecise because multiple factors influence recovery, including the site, mechanism, and severity of the injury as well as the sport and position that the athlete plays (71). Clinical assessment and physical examination are poor predictors of return to play (71,72). While the added utility of imaging has been questioned, most professional team physicians rely on MR imaging to help guide rehabilitation planning (4,73,74). Normal imaging results after injury are predictive of rapid recovery, while longer recovery times correlate with higher MR imaging grades, with injuries that demonstrate more structural damage taking longer to heal (70,73,75).

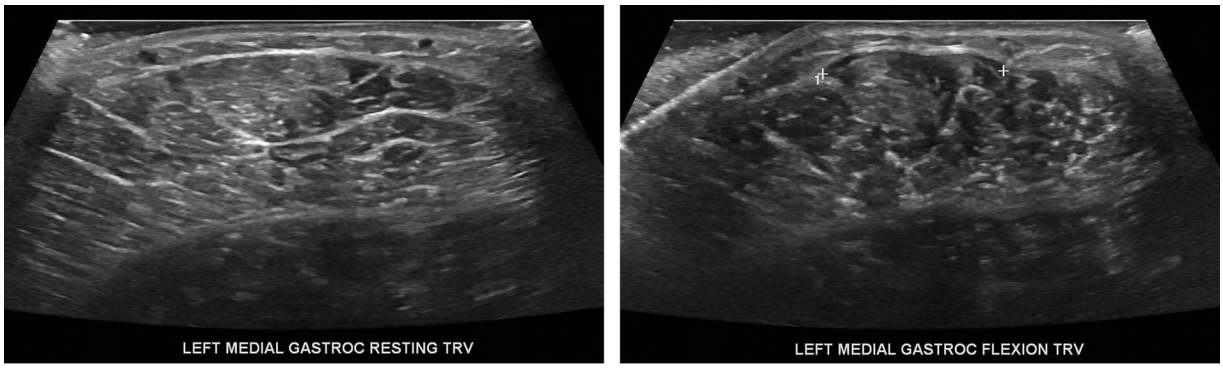

a. **b.**

Figure 32. Muscle hernia in a 27-year-old man with a palpable calf mass exacerbated by exercise involving ankle plantar flexion. **(a)** Transverse resting US image of the left calf appears normal. **(b)** Transverse US image during ankle flexion shows a contour change, with focal bulging of the medial gastrocnemius muscle (between cursors) related to incompetence of the overlying fascia.

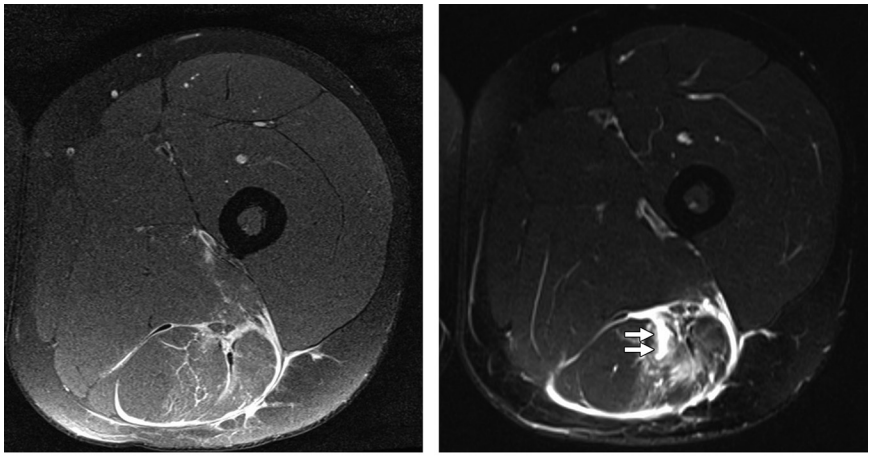

a. **b.**

Figure 33. Muscle strain followed by reinjury at the same site in a professional soccer player. **(a)** Axial proton-density–weighted fat-suppressed MR image of the left thigh after an acute sports injury shows a low-grade myotendinous strain of the hamstrings, with epimysial fluid tracking around the muscles and mild intramuscular edema. He returned to play 12 days later against the advice of his trainer and experienced acute pain while running. **(b)** Follow-up axial T2-weighted fat-suppressed MR image shows increased fluid in the muscle and a new region of architectural distortion with a fluid-filled void in the semimembranosus (arrows), indicating reinjury that is now moderate grade.

The literature regarding return to play is primarily based on hamstring injuries in young male professional athletes. As early as 1993, it was noted that injuries exhibiting complete transection, greater than 50% cross-sectional involvement, MTJ tearing, deep damage, and intramuscular fluid collections at MR imaging required longer rehabilitation than smaller, more superficial injuries without myotendinous disruption (76). Subsequent studies have also demonstrated a relationship between number of days lost and the percentage of the muscle's cross-sectional area and volume involved, length of MTJ signal intensity changes, and visible tendon damage (18,19,75,77).

Healing rates show considerable heterogeneity, even within the hamstring musculature; the biceps femoris takes longer to heal and is most prone to reinjury (70,77,78). Recovery times for quadriceps and calf injuries are similar to those of the hamstrings, whereas groin injuries tend to heal more quickly, but the number of studies focusing on these regions is limited (70). Little information is available regarding return to activity in recreational athletes, female athletes, children, the elderly, or patients with comorbidities.

Abnormal Healing

Dysfunction of satellite cells related to injury severity, inadequate immobilization, degraded immune response, aging, hypoperfusion, and/or altered local microenvironment leads to failure of the regeneration pathway, resulting in degeneration of damaged muscle and its replacement by fibrous, fatty, and/or metaplastic tissue

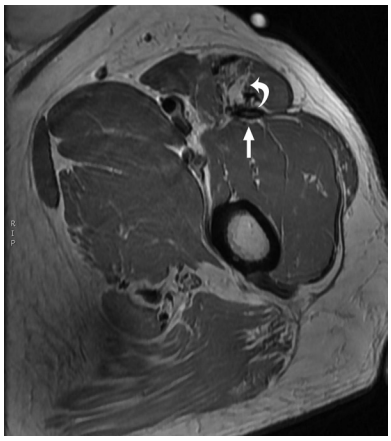

Figure 34. Abnormal healing in a 76-year-old man with a remote history of thigh strain. Axial T1-weighted MR image shows sequelae of remote injury of the rectus femoris muscle deep to the marker. There is fibrosis resulting in thickening at the posterior aponeurosis (straight arrow). Note the fatty replacement of the central muscle (curved arrow) related to muscle degeneration and tissue loss.

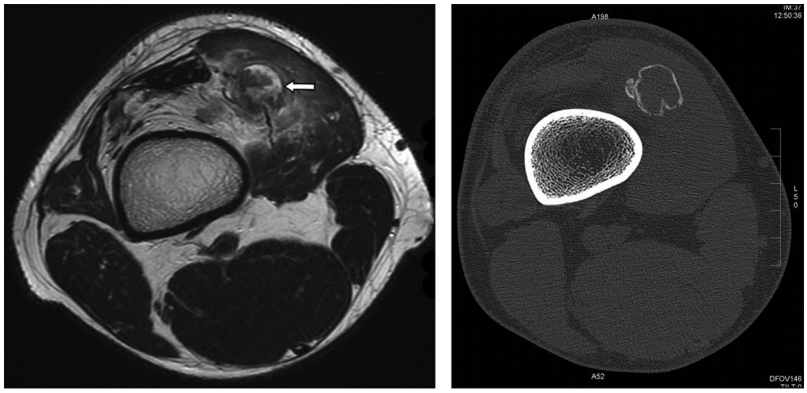

a. b.

Figure 35. Myositis ossificans in a professional soccer player who was kicked in the thigh 6 weeks earlier. **(a)** Axial T2-weighted MR image shows a poorly marginated heterogeneous mass in the vastus medialis (arrow), which disrupts the myotendinous tissue and is surrounded by poorly defined muscle edema/hemorrhage. There is a suggestion of a low-signal-intensity rim, suggestive of peripheral fibrosis or early ossification. **(b)** Axial CT image 2 weeks later clearly shows the characteristic peripheral rind of ossification pathognomonic for myositis ossificans. (Courtesy of Enrique Bosch, MD, Clinica Alemana, Santiago, Chile.)

(47,67). Repair of myotendinous injury is often incomplete, resulting in permanent deformity at the region of injury due to excess scar formation, visible as focal tendon thickening.

In the muscle, incomplete healing results in an admixture of fibrosis and regions of fatty replacement of damaged muscle, which can be difficult to appreciate at MR imaging without comparison to the contralateral side if scarring is minor (Fig 34). At US, areas of scarring appear as hyperechoic zones within the muscle (44). These areas of faulty repair exhibit increased stiffness and loss of compliance, which may result in long-term functional impairment.

Myositis Ossificans

Disordered satellite cell differentiation can cause intramuscular bone proliferation, a nonneoplastic aberration of repair termed *myositis ossificans* (40). Myositis ossificans is most common after direct muscle trauma, although burns, immobilization, and neurologic dysfunction can also incite its formation. Posttraumatic ossification most commonly affects the quadriceps, adductor, or brachialis musculature of children and young adults.

Myositis ossificans initially causes active vascular and cellular proliferation that appears as an ill-defined soft-tissue mass. Immature lesions may be intensely edematous and poorly defined, resembling an aggressive neoplasm, or may have a thick enhancing rim, mimicking an abscess (79). Intermediate lesions exhibit a predominantly cellular core of active fibroblasts, resembling nodular fasciitis (80), before developing better-defined margins and faint marginal calcifications, typically 2–4 weeks after injury. Such early calcifications are difficult to appreciate at MR imaging and are best demonstrated at CT (79).

Mature lesions, typically 6 or more weeks after injury, demonstrate the distinctive zonal organization of myositis ossificans, with a peripheral ring of mature ossification at its margins surrounding a central cellular core (81) (Fig 35). At US, acoustic shadowing develops at the osseous interface at this stage, obscuring the center of the lesion. With further maturation, the cellular central core evolves into mature fat-containing marrow that is clearly recognized at MR imaging.

Grading of Acute Muscle Injury

Initial Grading Systems

Early grading systems for muscle injury were based solely on clinical criteria and divided

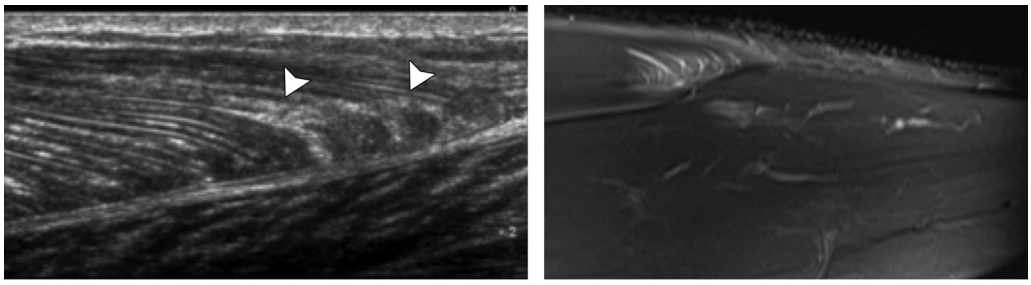

a. b.

Figure 36. Grade 1 strain injury in a 25-year-old female soccer player with acute onset of right calf pain during a match. **(a)** Longitudinal gray-scale US image of the right gastrocnemius shows echogenic foci oriented along the muscle fibers adjacent to the MTJ (arrowheads) without an intramuscular fluid collection, reflecting a grade 1 strain injury. In addition to foci of increased echogenicity, grade 1 strains can manifest with mild fiber irregularity, thinning, or waviness at US. **(b)** Coronal short inversion time inversion-recovery (STIR) MR image rotated to match the US image shows feathery high signal intensity in the muscle without architectural distortion.

muscle injuries into three grades (1,20,82). The advent of US and MR imaging allowed supplemental objective assessment of the extent and precise location of injury (Fig 36). Imaging-based grading systems for muscle injury based on the extent of cross-sectional involvement of muscle were initially developed using US, using somewhat variable percentages of involvement for deciding injury grade.

One popular US grading system categorized injuries involving less than 20% of the muscle as grade 1, those involving 20%–50% as grade 2, and those involving greater than 50% as grade 3 (20). Some authors have suggested that any fluid-filled gap in the muscle reflects a grade 2 injury, regardless of the percentage involvement, as it indicates a macroscopic tear. Recognition of symptomatic injuries lacking objective imaging findings resulted in the addition of a grade 0 category (44).

Initial MR imaging grading systems similarly relied on the pattern of muscle signal intensity alterations for grading, dividing injuries into three grades, with grade 1 injuries showing only edema, grade 2 injuries showing architectural distortion with intramuscular hemorrhage and gaps in the tissue, and grade 3 injuries denoting complete disruption of the MTJ. Subsequently, a grade 0 category was added for symptomatic injuries without MR imaging findings.

Unfortunately, these early three- or four-part grading systems lack sufficient precision and prognostic value, as injuries of various causes and different pathophysiologies are bundled together without sufficient emphasis on the underlying mechanism and precise location of structural damage (83).

Comprehensive Grading Systems

Recently, a plethora of comprehensive grading systems for muscle injury have been proposed to provide greater precision and more accurate prognostication (Table 2). In 2012, the Munich Muscle Injury Classification was developed by 15 international sports injury experts on the basis of their combined experience with over 400 thigh injuries in professional athletes (2). The Munich system separates muscle injuries into three categories: functional disorders, strain, and contusion. Strain injuries are subdivided into three semiquantitative grades based on the diameter of the injury, with structural tissue loss greater than 5 mm indicating at least a moderate-grade injury. The Munich system's introduction of several functional muscle disorders has proved problematic, as these lack strict definitions or imaging correlates, limiting reproducibility (20).

The Italian Society of Muscles, Ligaments, and Tendons (ISMuLT) classification is similar to the Munich system but includes a description of the longitudinal location of strain, separating involvement of the proximal, middle, or distal muscle. This separation is based on observations that proximal injuries at muscles such as the hamstrings and quadriceps take longer to heal, whereas at other muscles, such as the triceps, healing is more prolonged if the injury is distal (Fig 37) (51).

The British Athletics Muscle Injury Classification focuses on strain and divides it into five grades of severity—grade 0 (MR imaging negative) to grade 4 (complete tear)—based on a combination of clinical evaluation and MR imaging assessment of the cross-sectional area and length of the injury. This system also assigns a letter to each injury grade on the basis of whether the injury is localized to the epimysium/fascia, MTJ, or tendon, as recovery times are shortest for epimysial strain and longest if there is frank tendon damage (25) (Fig 38).

The Barcelona soccer team and Aspetar physicians have developed the MLG-R Classification, which divides injuries into direct and indirect, then subclassifies direct injuries into three grades according to longitudinal location (similar to

Table 2: Muscle Injury Grading Systems

Features	Clinical	Advent of Imaging	Munich Classification	Italian ISMuLT	British Athletics	Barcelona/Aspetar MLG-R
Grading criteria	Clinical only	Clinical and US/MR imaging	Clinical and US/MR imaging	Clinical and US/MR imaging	Clinical and MR imaging	Clinical and US/MR imaging (MR imaging preferred)
Mechanism of injury	Not separated	Not separated	Indirect functional Indirect strain Direct contusion Direct laceration	Indirect functional Indirect strain Direct contusion Direct laceration	Indirect strain Direct contusion	Indirect strain Direct contusion
Injury grade	Grades 1–3: 1= pain 2 = weakness or decreased range of motion 3 = disabled	Grades 0–3: 0 = imaging negative 1 = edema 2 = structural injury 3 = high-grade/complete tear	Strain grades 3a, 3b, and 4: 3a = <5 mm diameter 3b = >5 mm diameter 4 = >50% muscle diameter, visible MTJ tear or tendon avulsion	Strain grades 3a, 3b, and 4: 3a = <5 mm diameter 3b = >5 mm diameter 4 = >50% muscle diameter, visible MTJ tear or tendon avulsion	Strain grades 0–4: 0 = imaging negative 1 = CSA < 10%, length < 5 cm, diameter < 5 cm 2 = CSA 10%–50%, length 5–15 cm, diameter < 5 cm 3 = CSA > 50%, length > 15 cm, diameter > 5 cm 4 = full-thickness tear of muscle or tendon	Strain grades 0–4: 0 = imaging negative 1 = ≤10% CSA 2 = 11%–25% CSA 3 = 26%–49% CSA 4 = ≥50% CSA
Injury location	…	…	…	Proximal Middle Distal	A = myofascial B = myotendinous C = intratendinous	Strain: Proximal tendon Distal tendon Proximal MTJ Distal MTJ Peripheral Contusion: Proximal muscle Middle muscle Distal muscle R0 = initial injury R1 = first reinjury at site, etc

Note.—CSA = cross-sectional area; ISMuLT = Italian Society of Muscles, Ligaments, and Tendons; MLG-R = mechanism, location, grade, and reinjury.

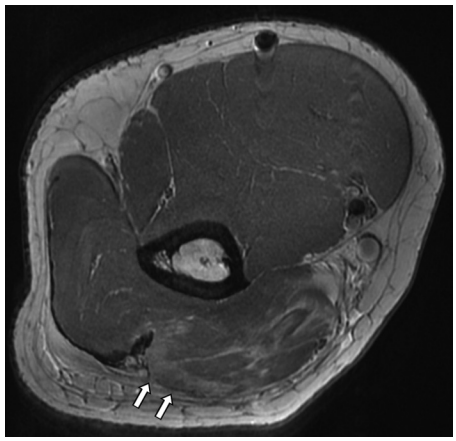

Figure 37. Myotendinous injury of the distal triceps in a 29-year-old male professional athlete. Axial proton-density–weighted MR image at the level of the right distal humerus shows moderate-grade injury of the medial and long heads of the triceps muscle, with areas of fiber tearing and architectural distortion abutting a partially torn MTJ (arrows). In contradistinction to the hamstrings and quadriceps, distal strains of the triceps take longer to heal than those located at the proximal MTJ.

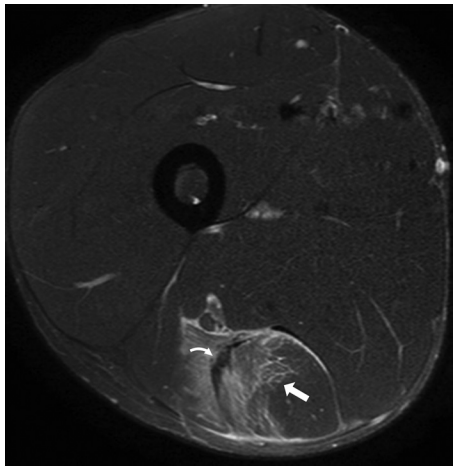

Figure 38. Strain injury of the long head of the biceps femoris with damage to the tendon in a 35-year-old male professional soccer player. Axial proton-density–weighted fat-suppressed MR image at the right midthigh shows a muscle strain at the biceps femoris (straight arrow). There is considerable intramuscular edema, but it does not violate the muscle architecture. Note that the aponeurotic tendon at the epicenter of the edema is thickened and edematous (curved arrow), reflecting intratendinous injury and indicating that it will take longer to heal. Mild edema is also seen in the short head biceps femoris muscle anterior to the tendon injury.

ISMuLT) and subclassifies indirect injuries by area involved and specific tissues injured (similar to British Athletics) (28,84). This system additionally stratifies strain into initial injury or reinjury at a site of prior tissue damage, reflecting the average 30% longer recovery time for reinjury at sites of preexisting tissue damage (28,84) (Fig 39).

Early studies assessing the utility of these comprehensive systems suggest that classifications incorporating mechanism, clinical assessment, and imaging findings reflecting the precise location and extent of injury improve prognostic accuracy (83,85).

Conclusion

Muscle injury is common and can take numerous forms, depending on the mechanism of injury and the acuity of the process. An understanding of the underlying anatomy and pathophysiology of muscle injuries helps one understand the varied imaging appearances of a range of different muscle injuries encountered in clinical practice (Table 3).

MR imaging, with its high spatial and contrast resolution, is ideally suited for imaging muscle trauma while allowing simultaneous assessment of adjacent osseous and articular structures. MR imaging plays a complementary role to US, which is more readily available and allows dynamic imaging of muscle trauma. MR imaging and US allow accurate diagnosis, objective assessment of injury severity, and precise localization of the sites of tissue damage, enabling detailed grading of injury severity.

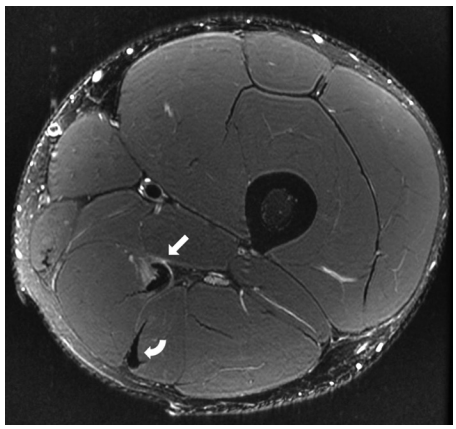

Figure 39. Reinjury at site of previous semimembranosus strain in an American football player. Axial proton-density–weighted fat-suppressed MR image of the left thigh shows evidence of a remote injury, characterized by thickening and fibrosis of the semimembranosus (straight arrow) and semitendinosus (curved arrow) tendons. There is mild edema in the muscle adjacent to the thickened tendon, related to an acute low-grade strain superimposed on chronic tissue damage. The MLG-R classification system assigns a numeric grade to the R suffix in strain injuries, indicating if there has been prior trauma to that site.

Grading systems for muscle injury are evolving rapidly. Radiologists involved in imaging of elite athletes need to become familiar with these newer systems, as imaging plays an increasingly

Table 3: Clinical and MR Imaging Features of Muscle Injuries

Cause	Injury	Clinical Features	Imaging Features
Indirect (stretching)			
Acute injury during eccentric exercise	Acute muscle strain	Immediate onset of pain at time of injury during activity	Edema maximal at an MTJ (junction of muscle and free tendon, around the intramuscular tendon, or at the epimysium) Normal muscle architecture in low-grade injury Architectural distortion of muscle in moderate- and high-grade injuries with fluid-filled gaps in muscle substance Tearing of tendon substance may be present
Sequela of old injury	Chronic muscle strain	Sequela of moderate- or high-grade injury	Architectural distortion localized at MTJ Tendon thickening and irregularity Adjacent muscle fibrosis or atrophy
Unaccustomed or excessive eccentric exercise	DOMS	Gradual onset of muscle pain several hours or days after activity	Edema of entire muscle or group of functionally similar muscles Independent of MTJ Normal muscle architecture Can persist for many weeks after activity
Direct (contact)			
Nonpenetrating blunt trauma	Contusion	Severity determined by force of impact Recovery time significantly shorter than for strain injury	Intramuscular hematoma and/or parenchymal hemorrhage at site of impact Independent of MTJ Signal intensity of hematoma changes with degradation of blood products Superficial edema and/or bone contusion may also be present
Penetrating trauma by a sharp object	Laceration	Clinically evident	Clearly demarcated linear defect in muscle Defect can contain blood, fluid, and/or gas
Chronic sequela of direct muscle trauma	Myositis ossificans	Intramuscular mass Pain, restricted range of movement	Variable appearance depending on maturity Immature lesion appears as ill-defined inflammatory mass that simulates intramuscular malignancy or abscess Mature lesion demonstrates characteristic shell of peripheral ossification best appreciated with CT
Disorders of connective tissue wrappers			
Acute elevation of compartment pressure	Acute compartment syndrome	Most common cause is fracture Arterial insufficiency	Enlargement of muscles in one or more compartments with loss of intramuscular fat planes Disordered tissue enhancement related to rhabdomyolysis and liquefaction
Exercise-related elevation of compartment pressure	CECS	Transient muscle pain, cramping, and tightness during exercise that resolve at end of activity	Mild muscle edema immediately after exercise that resolves within 30 minutes (can also be seen in asymptomatic persons) Normal muscle architecture
Fascial defect or insufficiency	Muscle hernia	Palpable mass that appears or enlarges during muscle contraction or upright positioning	Protruberant mass with signal intensity characteristics identical to those of normal muscle Mass more apparent with muscle contraction and upright posture Fascial defect/thinning may be visible
Degloving injury due to shearing at subcutaneous fat–fascia interface	Morel-Lavallée lesion	Palpable mass in area of prior injury Most common at lateral proximal thigh	Subcutaneous fluid collection adjacent to superficial fascia Often elliptical, elongated along plane of fascia Contains blood products of varying age, may contain fat globules

important role in diagnosis and management of the injured athlete.

Acknowledgment.—We thank Samuel Ward, PhD, for his guidance and assistance in preparing this material.

References

1. Guermazi A, Roemer FW, Robinson P, Tol JL, Regatte RR, Crema MD. Imaging of muscle injuries in sports medicine: sports imaging series. Radiology 2017;282(3):646–663.
2. Mueller-Wohlfahrt HW, Haensel L, Mithoefer K, et al. Terminology and classification of muscle injuries in sport: the Munich consensus statement. Br J Sports Med 2013;47(6):342–350.
3. Boutin RD, Fritz RC. MRI of musculotendinous injuries. I. "Non-strain" injuries. Curr Radiol Rep 2015;3:30.
4. Boutin RD, Fritz RC. MRI of musculotendinous injuries: what's new? II. Strain injuries. Curr Radiol Rep 2015;3:27.
5. Zaraiskaya T, Kumbhare D, Noseworthy MD. Diffusion tensor imaging in evaluation of human skeletal muscle injury. J Magn Reson Imaging 2006;24(2):402–408.
6. Aweid O, Del Buono A, Malliaras P, et al. Systematic review and recommendations for intracompartmental pressure monitoring in diagnosing chronic exertional compartment syndrome of the leg. Clin J Sport Med 2012;22(4): 356–370.
7. McCully KK, Argov Z, Boden BP, Brown RL, Bank WJ, Chance B. Detection of muscle injury in humans with 31-P magnetic resonance spectroscopy. Muscle Nerve 1988;11(3):212–216.
8. Benjamin M, Kaiser E, Milz S. Structure-function relationships in tendons: a review. J Anat 2008;212(3):211–228.
9. Oatis C. Biomechanics of skeletal muscle. In: Oatis C, ed. Kinesiology: mechanics and pathomechanics of human motion. 2nd ed. Philadelphia, Pa: Lippincott Williams & Wilkins, 2009; 49–51.
10. McMaster PE. Tendon and muscle ruptures: clinical and experimental studies on the causes and location of subcutaneous ruptures. J Bone Joint Surg Am 1933;15(3):705–722.
11. Costa AF, Di Primio GA, Schweitzer ME. Magnetic resonance imaging of muscle disease: a pattern-based approach. Muscle Nerve 2012;46(4):465–481.
12. Lieber RL, Fridén J. Clinical significance of skeletal muscle architecture. Clin Orthop Relat Res 2001;(383):140–151.
13. Shellock FG, Fukunaga T, Mink JH, Edgerton VR. Acute effects of exercise on MR imaging of skeletal muscle: concentric vs eccentric actions. AJR Am J Roentgenol 1991;156(4):765–768.
14. Fleckenstein JL, Canby RC, Parkey RW, Peshock RM. Acute effects of exercise on MR imaging of skeletal muscle in normal volunteers. AJR Am J Roentgenol 1988;151(2):231–237.
15. Lieber RL, Ward SR. Skeletal muscle design to meet functional demands. Philos Trans R Soc Lond B Biol Sci 2011;366(1570):1466–1476.
16. Palmer WE, Kuong SJ, Elmadbouh HM. MR imaging of myotendinous strain. AJR Am J Roentgenol 1999;173(3):703–709.
17. Lieber RL, Fridén J. Functional and clinical significance of skeletal muscle architecture. Muscle Nerve 2000;23(11):1647–1666.
18. Hayashi D, Hamilton B, Guermazi A, de Villiers R, Crema MD, Roemer FW. Traumatic injuries of thigh and calf muscles in athletes: role and clinical relevance of MR imaging and ultrasound. Insights Imaging 2012;3(6):591–601.
19. Feeley BT, Kennelly S, Barnes RP, et al. Epidemiology of National Football League training camp injuries from 1998 to 2007. Am J Sports Med 2008;36(8):1597–1603.
20. Grassi A, Quaglia A, Canata GL, Zaffagnini S. An update on the grading of muscle injuries: a narrative review from clinical to comprehensive systems. Joints 2016;4(1):39–46.
21. Shelly MJ, Hodnett PA, MacMahon PJ, Moynagh MR, Kavanagh EC, Eustace SJ. MR imaging of muscle injury. Magn Reson Imaging Clin N Am 2009;17(4):757–773, vii.
22. El-Khoury GY, Brandser EA, Kathol MH, Tearse DS, Callaghan JJ. Imaging of muscle injuries. Skeletal Radiol 1996;25(1):3–11.
23. Bencardino JT, Rosenberg ZS, Brown RR, Hassankhani A, Lustrin ES, Beltran J. Traumatic musculotendinous injuries of the knee: diagnosis with MR imaging. RadioGraphics 2000;20(Spec No):S103–S120.
24. Knudsen AB, Larsen M, Mackey AL, et al. The human myotendinous junction: an ultrastructural and 3D analysis study. Scand J Med Sci Sports 2015;25(1):e116–e123.
25. Pollock N, James SL, Lee JC, Chakraverty R. British Athletics Muscle Injury Classification: a new grading system. Br J Sports Med 2014;48(18):1347–1351.
26. Maquirriain J, Ghisi JP, Kokalj AM. Rectus abdominis muscle strains in tennis players. Br J Sports Med 2007;41(11):842–848.
27. Koulouris G, Connell D. Hamstring muscle complex: an imaging review. RadioGraphics 2005;25(3):571–586.
28. Valle X, Alentorn-Geli E, Tol JL, et al. Muscle injuries in sports: a new evidence-informed and expert consensus-based classification with clinical application. Sport Med 2017;47(7):1241–1253.
29. Lee JC, Healy J. Sonography of lower limb muscle injury. AJR Am J Roentgenol 2004;182(2):341–351.
30. Koh ES, McNally EG. Ultrasound of skeletal muscle injury. Semin Musculoskelet Radiol 2007;11(2):162–173.
31. Delgado GJ, Chung CB, Lektrakul N, et al. Tennis leg: clinical US study of 141 patients and anatomic investigation of four cadavers with MR imaging and US. Radiology 2002;224(1):112–119.
32. Chiavaras MM, Jacobson JA, Smith J, Dahm DL. Pectoralis major tears: anatomy, classification, and diagnosis with ultrasound and MR imaging. Skeletal Radiol 2015;44(2):157–164.
33. Gyftopoulos S, Rosenberg ZS, Schweitzer ME, Bordalo-Rodrigues M. Normal anatomy and strains of the deep musculotendinous junction of the proximal rectus femoris: MRI features. AJR Am J Roentgenol 2008;190(3):W182–W186.
34. Kassarjian A, Rodrigo RM, Santisteban JM. Intramuscular degloving injuries to the rectus femoris: findings at MRI. AJR Am J Roentgenol 2014;202(5):W475–W480.
35. Armstrong RB. Mechanisms of exercise-induced delayed onset muscular soreness: a brief review. Med Sci Sports Exerc 1984;16(6):529–538.
36. Shellock FG, Fukunaga T, Mink JH, Edgerton VR. Exertional muscle injury: evaluation of concentric versus eccentric actions with serial MR imaging. Radiology 1991;179(3):659–664.
37. Lieber RL, Fridén J. Morphologic and mechanical basis of delayed-onset muscle soreness. J Am Acad Orthop Surg 2002;10(1):67–73.
38. Cermak NM, Noseworthy MD, Bourgeois JM, Tarnopolsky MA, Gibala MJ. Diffusion tensor MRI to assess skeletal muscle disruption following eccentric exercise. Muscle Nerve 2012;46(1):42–50.
39. Fridén J, Sfakianos PN, Hargens AR, Akeson WH. Residual muscular swelling after repetitive eccentric contractions. J Orthop Res 1988;6(4):493–498.
40. Beiner JM, Jokl P. Muscle contusion injury and myositis ossificans traumatica. Clin Orthop Relat Res 2002;(403 suppl):S110–S119.
41. Thorsson O, Lilja B, Nilsson P, Westlin N. Immediate external compression in the management of an acute muscle injury. Scand J Med Sci Sports 1997;7(3):182–190.
42. Ueblacker P, Müller-Wohlfahrt HW, Ekstrand J. Epidemiological and clinical outcome comparison of indirect ('strain') versus direct ('contusion') anterior and posterior thigh muscle injuries in male elite football players: UEFA Elite League study of 2287 thigh injuries (2001-2013). Br J Sports Med 2015;49(22):1461–1465.
43. Swensen SJ, Keller PL, Berquist TH, McLeod RA, Stephens DH. Magnetic resonance imaging of hemorrhage. AJR Am J Roentgenol 1985;145(5):921–927.
44. Peetrons P. Ultrasound of muscles. Eur Radiol 2002;12(1):35–43.
45. Pathria MN, Boutin RD. Magnetic resonance imaging of muscle. In: Hodler J, von Schulthess G, Zollikofer C, eds. Musculoskeletal diseases 2009-2012. Milan, Italy: Springer, 2009; 57–62.
46. Boutin R, Pathria M. Magnetic resonance imaging of muscle. In: Hodler J, von Schulthess G, Zollikofer CL, eds. Muscu-

loskeletal diseases 2013-2016. Milan, Italy: Springer-Verlag, 2013; 161–170.
47. Järvinen TA, Järvinen TL, Kääriäinen M, Kalimo H, Järvinen M. Muscle injuries: biology and treatment. Am J Sports Med 2005;33(5):745–764.
48. Boutin RD, Fritz RC, Steinbach LS. Imaging of sports-related muscle injuries. Radiol Clin North Am 2002;40(2):333–362, vii.
49. May DA, Disler DG, Jones EA, Balkissoon AA, Manaster BJ. Abnormal signal intensity in skeletal muscle at MR imaging: patterns, pearls, and pitfalls. RadioGraphics 2000;20(Spec No):S295–S315.
50. Mellado JM, Pérez del Palomar L, Díaz L, Ramos A, Saurí A. Long-standing Morel-Lavallée lesions of the trochanteric region and proximal thigh: MRI features in five patients. AJR Am J Roentgenol 2004;182(5):1289–1294.
51. Maffulli N, Del Buono A, Oliva F, et al. Muscle injuries: a brief guide to classification and management. Transl Med UniSa 2014;12(4):14–18.
52. McNee M, Levine B, Plotkin B, Motamedi K. Sonography of muscle: normal findings and spectrum of abnormalities. Curr Radiol Rep 2015;3:5.
53. Weng KH, Tzeng WS, Shu GH, Lo CW, Chen CK. Magnetic resonance imaging of compartment syndrome: report of three cases. J Radiol Sci 2013;38:65–70.
54. Oliva F, Via AG, Kiritsi O, Foti C, Maffulli N. Surgical repair of muscle laceration: biomechanical properties at 6 years follow-up. Muscles Ligaments Tendons J 2014;3(4):313–317.
55. Rominger MB, Lukosch CJ, Bachmann GF. MR imaging of compartment syndrome of the lower leg: a case control study. Eur Radiol 2004;14(8):1432–1439.
56. O'Dwyer HM, Al-Nakshabandi NA, Al-Muzahmi K, Ryan A, O'Connell JX, Munk PL. Calcific myonecrosis: keys to recognition and management. AJR Am J Roentgenol 2006;187(1):W67–W76.
57. McMahon CJ, Wu JS, Eisenberg RL. Muscle edema. AJR Am J Roentgenol 2010;194(4):W284–W292.
58. Andreisek G, White LM, Sussman MS, et al. T2*-weighted and arterial spin labeling MRI of calf muscles in healthy volunteers and patients with chronic exertional compartment syndrome: preliminary experience. AJR Am J Roentgenol 2009;193(4):W327–W333.
59. Pedowitz RA, Hargens AR, Mubarak SJ, Gershuni DH. Modified criteria for the objective diagnosis of chronic compartment syndrome of the leg. Am J Sports Med 1990;18(1):35–40.
60. Ringler MD, Litwiller DV, Felmlee JP, et al. MRI accurately detects chronic exertional compartment syndrome: a validation study. Skeletal Radiol 2013;42(3):385–392.
61. Amendola A, Rorabeck CH, Vellett D, Vezina W, Rutt B, Nott L. The use of magnetic resonance imaging in exertional compartment syndromes. Am J Sports Med 1990;18(1):29–34.
62. Bong MR, Polatsch DB, Jazrawi LM, Rokito AS. Chronic exertional compartment syndrome: diagnosis and management. Bull Hosp Jt Dis 2005;62(3-4):77–84.
63. Roberts A, Franklyn-Miller A. The validity of the diagnostic criteria used in chronic exertional compartment syndrome: a systematic review. Scand J Med Sci Sports 2012;22(5):585–595.
64. Mellado JM, Pérez del Palomar L. Muscle hernias of the lower leg: MRI findings. Skeletal Radiol 1999;28(8):465–469.
65. Beggs I. Sonography of muscle hernias. AJR Am J Roentgenol 2003;180(2):395–399.
66. Saifuddin A, Tyler P, Hargunani R. Pathology of the soft tissues. In: Musculoskeletal MRI. 2nd ed. Boca Raton, Fla: CRC, 2008; 792.
67. Yoseph B, Soker S. Redefining the satellite cell as the motor of skeletal muscle regeneration. J Sci Appl Biomed 2015;3(5):76–82.
68. Järvinen TA, Järvinen M, Kalimo H. Regeneration of injured skeletal muscle after the injury. Muscles Ligaments Tendons J 2014;3(4):337–345.
69. Kerkhoffs GMMJ, van Es N, Wieldraaijer T, Sierevelt IN, Ekstrand J, van Dijk CN. Diagnosis and prognosis of acute hamstring injuries in athletes. Knee Surg Sports Traumatol Arthrosc 2013;21(2):500–509.
70. Hallén A, Ekstrand J. Return to play following muscle injuries in professional footballers. J Sports Sci 2014;32(13):1229–1236.
71. Rubin DA. Imaging diagnosis and prognostication of hamstring injuries. AJR Am J Roentgenol 2012;199(3):525–533.
72. Reiman MP, Loudon JK, Goode AP. Diagnostic accuracy of clinical tests for assessment of hamstring injury: a systematic review. J Orthop Sports Phys Ther 2013;43(4):223–231.
73. Ekstrand J, Askling C, Magnusson H, Mithoefer K. Return to play after thigh muscle injury in elite football players: implementation and validation of the Munich Muscle Injury Classification. Br J Sports Med 2013;47(12):769–774.
74. Reurink G, Brilman EG, de Vos RJ, et al. Magnetic resonance imaging in acute hamstring injury: can we provide a return to play prognosis? Sports Med 2015;45(1):133–146.
75. Ekstrand J, Healy JC, Waldén M, Lee JC, English B, Hägglund M. Hamstring muscle injuries in professional football: the correlation of MRI findings with return to play. Br J Sports Med 2012;46(2):112–117.
76. Pomeranz SJ, Heidt RS Jr. MR imaging in the prognostication of hamstring injury: work in progress. Radiology 1993;189(3):897–900.
77. Slavotinek JP, Verrall GM, Fon GT. Hamstring injury in athletes: using MR imaging measurements to compare extent of muscle injury with amount of time lost from competition. AJR Am J Roentgenol 2002;179(6):1621–1628.
78. Ekstrand J, Hägglund M, Waldén M. Epidemiology of muscle injuries in professional football (soccer). Am J Sports Med 2011;39(6):1226–1232.
79. Shirkhoda A, Armin AR, Bis KG, Makris J, Irwin RB, Shetty AN. MR imaging of myositis ossificans: variable patterns at different stages. J Magn Reson Imaging 1995;5(3):287–292.
80. Kransdorf MJ, Meis JM, Jelinek JS. Myositis ossificans: MR appearance with radiologic-pathologic correlation. AJR Am J Roentgenol 1991;157(6):1243–1248.
81. Kransdorf MJ, Murphey MD. Imaging of soft-tissue musculoskeletal masses: fundamental concepts. RadioGraphics 2016;36(6):1931–1948.
82. Chan O, Del Buono A, Best TM, Maffulli N. Acute muscle strain injuries: a proposed new classification system. Knee Surg Sports Traumatol Arthrosc 2012;20(11):2356–2362.
83. Hamilton B, Valle X, Rodas G, et al. Classification and grading of muscle injuries: a narrative review. Br J Sports Med 2015;49(5):306.
84. FCBarcelona. Muscle injuries clinical guide 3.0. Aspetar Sport Med J 2015;(January):10–14.
85. Patel A, Chakraverty J, Pollock N, Chakraverty R, Suokas AK, James SL. British Athletics Muscle Injury Classification: a reliability study for a new grading system. Clin Radiol 2015;70(12):1414–1420.